Wageningen Academic Publishers
Bastiaanse Communication
Beneficial Microbes

Host and gut microbial metabolism of Bifidobacterium longum-fermented rice bran in healthy mice and bioavailability of antimicrobial and cancer-protective compounds

Journal:	*Beneficial Microbes*
Manuscript ID	Draft
Manuscript Type:	Research article
Date Submitted by the Author:	n/a
Complete List of Authors:	Nealon, Nora Jean; Colorado State University, Environmental and Radiological Health Sciences Parker, Kristopher; Colorado State University, Environmental and Radiological Health Sciences Lahaie, Paige; Colorado State University, Environmental and Radiological Health Sciences Ibrahim, Hend; Colorado State University, Environmental and Radiological Health Sciences; Zagazig University, Faculty of Medicine Maurya, Akhilendra; University of Colorado, Skaggs School of Pharmacy and Pharmaceutical Sciences Raina, Komal; University of Colorado, Skaggs School of Pharmacy and Pharmaceutical Sciences; South Dakota State University, Department of Pharmaceutical Sciences Ryan, Elizabeth; Colorado State University, Environmental and Radiological Health Sciences; University of Colorado Cancer Center, Division of Cancer Control and Prevention
Keywords:	Food, Microbiome, Metabolites, Fermentation, Colon
Note: The following files were submitted by the author for peer review, but cannot be converted to PDF. You must view these files (e.g. movies) online.	
supplementary_material.tar.gz	

SCHOLARONE™
Manuscripts

Host and gut microbial metabolism of *Bifidobacterium longum*-fermented rice bran in healthy mice and bioavailability of antimicrobial and cancer-protective compounds.

N.J. Nealon*[1,2], K.D. Parker*[1], P. Lahaie[1], H. Ibrahim[1.3], A.K. Maurya[4], K. Raina[4,5], E.P. Ryan+[1,2,6]

[1]Department of Environmental and Radiological Health Sciences, College of Veterinary Medicine and Biomedical Sciences, Colorado State University, Fort Collins, CO, USA, 80521

[2]Program in Cellular and Molecular Biology, Colorado State University, Fort Collins, CO, USA, 80521

[3] Zagazig University, Department of Medical Biochemistry, Faculty of Medicine, Zagazig, Egypt, 44511

[4]Skaggs School of Pharmacy and Pharmaceutical Sciences, University of Colorado Denver-Anschutz Medical Campus, Aurora, CO, USA, 80045

[5]Department of Pharmaceutical Sciences, South Dakota State University, Brookings, SD, USA, 57007

[6]University of Colorado Cancer Center, Division of Cancer Control and Prevention, Aurora, CO, USA, 80045

*Authors contributed equally to the preparation of this manuscript.

+Corresponding author
Elizabeth P. Ryan, PhD
Colorado State University
College of Veterinary Medicine and Biomedical Sciences
1617 Campus Delivery
Fort Collins, CO, 80521
1-970-491-1536
e.p.ryan@colostate.edu

Running Header
Murine metabolism of *B. longum*-fermented rice bran for gut health.

For Peer Review

Abstract

Food fermentation by native gut probiotics has historical foundations for gut health promotion. Metabolic comparisons of fermented foods alongside the non-fermented forms have been largely unexplored using non-targeted metabolomics and thus merit evaluation before and after exposure to the gastrointestinal tract. This study investigated gut microbiota composition along with food, host, and microbial derived metabolites in the colon and systemic circulation of healthy mice following dietary intake of fermented versus non-fermented rice bran. Adult male BALB/c mice were fed a control diet or one of two experimental diets containing 10% w/w rice bran fermented with *Bifidobacterium longum* or 10% w/w non-fermented rice bran for 15 weeks. Metabolomics of each study diet (food), the murine colon and whole blood were analysed in concert with 16S amplicon sequencing of faecal, caecum, and colon samples. Principal components analysis of taxonomy-independent murine microbiota composition displayed marked separation between control and both experimental diet groups. This separation was apparent for all biological sample types, although faecal microbiomes were noticeably distinct from the caecum and colon. Mice in both experimental diet groups exhibited largely similar bacterial composition with identification of only two differentially abundant sequence variants- represented by *Roseburia* and Clostridiales. A total of 530 small molecules including 39% amino acids and 21% lipids were revealed through differential abundance testing across food, colon, and blood matrices. The amino acid metabolite, N-delta-acetylornithine, was notably significant for increased bioavailability by *B. longum* rice bran fermentation when compared to non-fermented rice bran across food, colon, and blood metabolomes. These findings support that dietary intake of rice bran fermented with *B. longum* modulates multiple metabolic pathways associated with antimicrobial actions and cancer prevention in the host via gut microbial metabolism despite minimal differences in gut microbiota composition when compared to non-fermented rice bran.

Keywords

Food, fermentation, microbiome, metabolites, colon

Introduction

Rice bran, the outer coating of brown rice, contributes the prebiotic, phytochemical and nutritional health benefits of whole grain brown rice. Numerous studies performed in humans and animals have shown colonic health and disease protective functions of a diet rich in rice bran (Henderson *et al.*, 2012a; Henderson *et al.*, 2012b; Lei *et al.*, 2016; Sheflin *et al.*, 2017; Sheflin *et al.*, 2015; Yang *et al.*, 2015). Metabolite profiling of heat-stabilised rice bran has revealed a large suite of bioactive compounds including various amino acids, small peptides, lipids, nucleotides, vitamins and cofactors, and plant phytochemicals available in digestible and non-digestible forms to the host (Zarei *et al.*, 2017). Many rice bran components have previously-reported roles in slowing tumour and pathogen growth *via* altering cell proliferation, combating oxidative stress, reducing inflammation and modulating the gut microbiome and metabolism (Fabian and Ju, 2011; Law *et al.*, 2017; So *et al.*, 2016; Sohail *et al.*, 2017). Rice bran components have also shown capacity for fermentation by gut commensal microbes (Sheflin *et al.*, 2017; Tuncil *et al.*, 2018). Emerging evidence supports that rice bran components modulate host and gut microbial metabolism to benefit enterocytes and the mucosal immune system (Brown *et al.*, 2017; Si *et al.*, 2018; Yang *et al.*, 2015; Zarei *et al.*, 2017). Genome sequencing of the faecal microbial communities and identification of small molecule profiles using metabolomics are promising tools to evaluate the effects of dietary interventions broadly (Bazanella *et al.*, 2017; Derkach *et al.*, 2017; Hernandez-Alonso *et al.*, 2017; Lee *et al.*, 2017; McIntosh *et al.*, 2017; Tovar *et al.*, 2017; Vandeputte *et al.*,

For Peer Review

2017), and were previously utilised for rice bran (Brown *et al.*, 2017; Henderson *et al.*, 2012a; Sheflin *et al.*, 2017; Sheflin *et al.*, 2015; Si *et al.*, 2018). However, these studies have not yet advanced our understanding of how rice bran fermentation impacts the colon tissue microbiome and the availability of the fermented food microbial-metabolic components to the colon and systemic circulation.

Few studies have evaluated the effects of fermented foods on healthy gut microbiomes (Cowan *et al.*, 2014; Zheng *et al.*, 2015), and to the best of the authors' knowledge, no studies currently provide a direct comparison to the non-fermented form of the same food type. Globally, lactic acid bacteria (LAB) are the widest order of microbes involved in food fermentation (Pessione and Cirrincione, 2016), and a variety of LAB, existing as part of the native gut microbiome, confer benefits to their host. *Bifidobacterium* represents another important genus of native gut probiotics that were shown to increase in relative percentages after 28 days of rice bran consumption (30g/day) by healthy adults (Sheflin *et al.*, 2015). In a related study with daily rice bran intake by adult colorectal cancer survivors, favourable modulations were captured in the stool metabolome, including shifts in fatty acid, branched chain amino acid, and B-vitamin metabolism (Brown *et al.*, 2017; Sheflin *et al.*, 2017). Multiple strains of *Bifidobacterium* have been tested in food fermentation and exhibited health effects related to increased production of short chain and branched chain fatty acids that are critical for normal colonocyte function (Bunesova *et al.*, 2016; Celiberto *et al.*, 2017; Gagnon *et al.*, 2015; Kim *et al.*, 2018; Phoem *et al.*, 2015).

This study aimed to distinguish host and microbe metabolic impacts of consuming dietary rice bran fermented with *Bifidobacterium longum* from the effects of consuming rice bran or a nutrient-matched control diet. Daily intake of *B. longum*-fermented rice bran for 15-weeks in healthy mice was hypothesised to elicit changes to host and intestinal microbiome metabolism and result in differences between bioactive metabolites in colon tissue and blood. This study used next-generation sequencing approaches to characterise murine caecum, colon, and faecal microbiomes and non-targeted metabolomics to determine metabolite profiles of study diets (food), colon tissue, and whole blood metabolomes of mice consuming each study diet. Multivariate statistical approaches were utilised to assess differential abundance of bacterial sequence variants and differential production of bioactive compounds with previously reported cancer-protective and antimicrobial functions. Exploiting both microbial sequencing and metabolomic platforms provided a thorough and sensitive analysis for revealing *B. longum*-fermented rice bran influences on gut microbiome metabolism and bioavailability of disease protective compounds.

Materials and methods

Rice bran and food fermentation

Ri300 heat-stabilised rice bran was purchased from Rice Bran Technologies (Sacramento, CA, USA). Ten kilograms of rice bran was thoroughly mixed with 10 litres of $1.5x10^8$ cells/mL of *Bifidobacterium longum (B. longum)* ATCC-55813 (American Type Culture Collection, Manassas, VA, USA) suspended in milliQ water (Millipore Corporation, Burlington, MA, USA). The mixture was placed in a sealed stainless-steel pot and incubated at 37^0C. After 48hrs, the resultant slurry was harvested at room temperature, and frozen at -20^0C until lyophilisation.

Mouse diet preparation and composition

B. longum-fermented rice bran was thawed and lyophilised overnight using a Labconco Freezone 4.5 Litre Freeze Dry System attached to an Edwards RV5 vacuum pump (Marshall Scientific, Hampton, NH, USA). Mouse diets were prepared as previously described using AIN-93 purified components as the control diet (Kumar *et al.*, 2012). The

For Peer Review

heat-stabilised rice bran and the *B. longum*-fermented rice bran was incorporated at 10% w/w into the diets at Envigo (Madison, WI, USA). Diets were matched for macronutrient and micronutrient contents with compositions listed in Table 1. Briefly, the control diet (TD.160791) was composed of four percent w/v corn oil, casein, L-cystine, corn starch, maltodextrin, sucrose, cellulose, mineral and vitamin mix, choline bitartrate, and TBHQ (Tertiary butyl-hydroquinone) antioxidant. The 10% w/w heat-stabilised rice bran diet and 10% w/w *B. longum*-fermented rice bran diet were adjusted across ingredients to account for nutrients supplied by the rice bran. Prior to animal feeding, diets were irradiated and determined to be free of pathogens and microbial toxins using standardised tests for anaerobic plate counts, coliform counts, *Escherichia coli* counts, mould counts, yeast counts, mesophilic aerobic spore counts, mesophilic anaerobic spore counts, and *Salmonella* counts.

Table 1. Composition of mouse diets for each study group.

Constituents (g/kg)	**Control**	**10% Rice bran**	**10% *B. longum*-fermented rice bran**
Casein	140.0	125.0	125.0
L-Cystine	1.8	1.8	1.8
Corn Starch	465.692	422.692	422.692
Maltodextrin	155.0	155.0	155.0
Sucrose	95.0	102.312	102.312
Corn Oil	40.0	19.0	19.0
Cellulose	50.0	29.0	29.0
Mineral Mix (with calcium and phosphate)	35.0	0	0
Mineral Mix (without calcium and phosphate)	0	13.388	13.388
Calcium Phosphate, Dibasic	0	7.5	7.5
Calcium Carbonate	0	6.8	6.8
Vitamin Mix	15.0	15.0	15.0
Choline Bitartrate	2.5	2.5	2.5
TBHQ, Antioxidant[1]	0.008	0.008	0.008
Rice bran	0	100.0	0
B. longum-fermented rice bran	0	0	100.00

[1]TBHQ: Tertiary butyl-hydroquinone

Ethics statement

Animal experiments were done under institutional guidelines using approved Institutional Animal Care and Use Committee (IACUC) protocol and an Inter-Institutional Agreement with Colorado State University.

Animal study design and sample collection

Animals were maintained in a specific-pathogen free (SPF) animal housing facility in UC Denver-Anschutz Medical Campus and monitored under an active Sentinel Monitoring Program. Mice were kept under standard conditions in SPF-ventilated isolators with built in systems for free access to water. Pellet diet was added in cage feeders and mice had free access to it. Six-week old male BALB/c mice (Charles River Laboratories) were fed a control AIN-93 pellet diet for a one-week acclimatisation period and then switched to rice bran (n=4), *B. longum*-fermented rice bran (n=4) or maintained on a control diet (n=5) for 15 weeks. During the 15-week feeding phase, faecal samples for each diet group were collected as a function of time for the following time points: 48 hours after diet intervention (considered week one), and thereafter on two, six, ten and fourteen weeks after diet intervention. Throughout the study, weekly body weight, diet consumption, and general health of mice was recorded. To avoid cross contamination of microbiota between different groups, only cages of one particular sub-group were opened under aseptic conditions in an animal transfer station at a given time. At the end of 15-week feeding phase (time of sacrifice), animals were subjected to CO2 asphyxiation and then euthanised by exsanguination. Whole blood was collected in

For Peer Review

BD vacutainer K2 EDTA coated tubes and stored at -80°C. Caecum and its contents were collected, snap frozen, and stored at -80°C until later use. The entire colon was excised from the caecum onwards to the distal end and cut open longitudinally along its main axis. Swab samples were collected from the proximal and lower portion of the distal colon and used for microbiome analysis. Next, colons were gently flushed with ice cold saline solution and cleaned with a fine brush to remove remnants of colonic contents. Approximately 2-3mm slivers of clean colon tissue from proximal and distal ends were cut, snap frozen, and stored at -80°C until later use for metabolomics analysis. An overview of the study design and experimental timeline is depicted in Figure 1.

Sample processing, DNA extraction, and 16S rRNA amplicon protocols

Lyophilised faecal samples and thawed tissue were homogenised and 50 mg/sample were used for DNA extraction with the MoBio PowerSoil Kit (MoBio Laboratories Inc., Solana Beach, CA, USA) following manufacturer protocols. Extracted DNA samples were stored at -20^{0}C until concentration and quality-checking on a NanoDrop 2000 (Thermo-Fisher Scientific, Lafayette, CO, USA). Amplification of prokaryotic 16S rRNA and amplicon sequencing on the Illumina MiSeq platform followed the standards outlined by the Earth Microbiome Project (Caporaso *et al.*, 2012; Caporaso *et al.*, 2011). PCR conditions included one initial cycle of 15 minutes DNA denaturation at 95^{0}C followed by 34 cycles of a 30-second DNA denaturation at 94C followed by 90 seconds of primer annealing at 92^{0}C, and one minute of DNA polymerization at 72^{0}C. All amplified samples were then subjected to a 10-minute extension at 72^{0}C. To confirm amplification prior to sequencing, all PCR products were run on a 1.5% agarose gel (BioRad, Hercules, CA) and visualized using 1µL Ethidium Bromide (Thermo-Fisher Scientific, Lafayette, CO) with PCR-grade water as a negative control. Prior to DNA library preparation, PCR products were purified using solid-phase reversible immobilization magnetic beads and quantified on a Cytation3 plate reader (BioTek Instruments Inc., Winooski, VT) using fluorimetry with sybr green tags (Kapa Biosystems Wilmington, MA). The pooled library was created with 50ng of DNA/sample and sequenced on an Illumina MiSeq (Illumina Inc., San Diego, CA) with 15% PhiX mock library to reduce discrepancies in read clustering and processed using the Illumina V2 500 cycle kit (2 x 250/250 paired-end reads). The V4 hypervariable region of 16S rRNA was targeted with the 515F/806R (Parada/Aprill) primer pair (Parada *et al.*, 2016; Walters *et al.*, 2016). Sequence for the 515F Parada forward primer: GTGYCAGCMGCCGCGGTAA; sequence for the 806R Aprill reverse primer: GGACTACNVGGGTWTCTAAT.

Sequence read denoising, dereplication, and chimera filtering

A total of 9,121,905 raw single-end FASTQ formatted forward sequence reads represented by 273 samples were imported into the Quantitative Insights Into Microbial Ecology 2 (QIIME 2) framework (Caporaso *et al.*, 2010). The cutadapt plugin was employed to trim any reads with a 5' match to the forward primer sequence (Martin, 2011). A feature table comprised of sequence variant (SV) absolute abundances for each sample was inferred from trimmed reads using the Divisive Amplicon Denoising Algorithm 2 (DADA2) pipeline (Callahan *et al.*, 2016). Representative sequences for each SV were also selected by DADA2. The following parameters were input into the dada2 plugin: chimera detection and removal using the consensus method (default); read truncation at the first position with a q-score less than or equal to two (default); reads were discarded if they exceeded a maximum expected error of two (default); any reads shorter than 248bp were discarded (user-input); the number of reads used to train the error model were increased to 10,000,000. In the context of this article, the term feature is interchangeable with sequence variant (i.e. feature = SV). Summary

For Peer Review

statistics and quality plots for raw and trimmed sequence reads were visualised using the demux plugin (Greg Caporaso). Feature table details were visualised using the feature-table plugin (McDonald *et al.*, 2012a). The manifest used for importing reads from FASTQ files into QIIME 2 was constructed in R version 3.5.2 (Team, 2018).

Sequence variant processing

Taxonomic identities for SV representative sequences were assigned with Naïve Bayes classifiers independently trained on 99% OTU reference collections from either Greenegenes 13_8 or SILVA 132 marker gene databases (DeSantis *et al.*, 2006; Glockner *et al.*, 2017; McDonald *et al.*, 2012b; Quast *et al.*, 2013; Yilmaz *et al.*, 2014). Reference collections used for classifier training were bound by the 515F/806R (Parada/Apprill) primer pair and trimmed to 248bp to reflect the length of SV representative sequences present in the dataset analysed here. This trimming step was previously shown to improve quality of resolution and confidence of assignment for 16S amplicon data (Bokulich *et al.*, 2018). The feature-classifier plugin was employed for training classifiers and assigning taxonomy and the confidence threshold for limiting taxonomic depth was increased to 0.75 (Bokulich *et al.*, 2018). The raw feature table, representative sequence file, and taxonomy tables were exported from QIIME 2 for further processing in R (Bokulich *et al.*, 2018; Team, 2018). Prior to import, the feature table was converted from BIOM to classic tab-delimited format using the biom-format Python package (McDonald *et al.*, 2012a). Following import into R, a master table comprised of hashed feature IDs with corresponding representative sequences, full and truncated Greengenes and SILVA taxonomic lineages, and raw absolute abundances for all features within all samples was constructed using base R in combination with package dplyr (Hadley Wickham, 2018). This master table served as the entry point for all downstream processing (Data File S1). Potential contaminant features assigned by either Greengenes or SILVA databases as chloroplast, mitochondria, eukaryote, or unassigned kingdom were removed from the master table using R package dplyr. Samples exhibiting excess of five percent relative abundance of contaminant features or samples with total absolute feature abundance fewer than 400 (considered to have been poorly sequenced) were removed from the master table. The processed master table was subset to create three tables with the samples needed for analyses presented here (Data Files S2, S3, S4). Samples analysed included 16 negative controls and 41 experimental samples represented by 13 caecum samples, 13 colon samples (six distal and seven proximal), and 15 faecal samples. For any subset table, features with total absolute abundance of less than two across subset samples were removed. The relative abundance of SVs assigned by both Greengenes and SILVA classifiers to the genus *Bifidobacterium* were visualised using base R and packages dplyr, ggplot2, ggpubr, and reshape2 (Hadley Wickham, 2018; Kassambara, 2018; Team, 2018; Wickham, 2007; 2016). Qualitative comparisons of taxonomy-independent microbiota composition (i.e. composition of all features in a given sample) proceeded using the compositional data analysis paradigm with count zero replacement prior to a ratio transformation to remove the simplex constraint inherent to amplicon sequencing data (Gloor *et al.*, 2017). Zero counts for features were imputed using the count zero multiplicative (CZM) method from R package zCompositions with a threshold of 0.5 and a delta of 0.65 (both defaults) (Palarea-Albaladejo and Martín-Fernández, 2015). The CZM function adjusts respective non-zero counts following simple multiplicative replacement for all zero counts (Martín-Fernández *et al.*, 2014; Palarea-Albaladejo and Martín-Fernández, 2015). CZM adjusted absolute abundances were transformed using the centred log-ratio (clr) transformation followed by ordination with principal components analysis (PCA). PCA plots were constructed using base R along with packages dplyr, ggbiplot, ggplot2, ggpubr, and grid (Hadley Wickham, 2018; Kassambara, 2018; Team, 2018; Vu, 2011; Wickham, 2016). Differential abundance testing of SVs

For Peer Review

between study diets was performed using the ALDEx2 package incorporated into R via the package BiocManager from the Bioconductor suite (Fernandes *et al.*, 2013; Fernandes *et al.*, 2014; Gentleman *et al.*, 2004; Huber *et al.*, 2015; Morgan, 2018). Testing was conducted as follows: 1000 Monte Carlo (MC) instances of the Dirichlet distribution for each sample were generated from subset tables containing absolute abundance data; clr transformation was then applied over each MC instance; *P*-values were produced using the non-parametric Wilcoxon rank-sum test (also called the Mann-Whitney *U* test) to compare each feature's clr values between two groups (H.B. Mann, 1947; Wilcoxon, 1945); *P*-values were adjusted for multiple comparisons using the Benjamani-Hochberg procedure to control for false discovery rate (FDR) resulting in *q*-values (Yoav Benjamini, 1995); *P*-values and *q*-values for each feature were averaged across all MC instances to yield expected *P*-values and *q*-values; any SV with an expected *q*-value less than 0.1 was deemed significant. Colours and colour schemes for all microbiome figures were selected using ColorBrewer 2.0 (Harrower and Brewer, 2003). The reader is referred to the online version of this article for the interpretation of figures in full colour.

Computational details for microbiome analyses

Microbiome analyses were performed on MacOS Mojave 10.14.2, running versions: biom-format 2.1.7, Conda 4.5.12, QIIME 2 2018.11.0, Python 3.6.5, R 3.5.2 'Eggshell Igloo', R Studio 1.1.463, and R package versions: ALDEx2 1.14.0, BiocManager 1.30.4, dplyr 0.7.8, ggbiplot 0.55, ggplot2 3.1.0, ggpubr 0.2, grid 3.5.2, reshape2 1.4.3, zCompositions 1.1.2.

Availability of microbiome data and analytical materials

The amplicon sequence data supporting the conclusions of this manuscript are available via NCBI SRA BioProject Accession PRJNA516457. Sample metadata are available in Metadata File S1. All code for analysis conducted in QIIME 2 is found in Code S1. The R code to create the manifest for importing FASTQ files into QIIME 2 is found at the beginning of Code S1. See Code S2 for all R code executed following analysis in QIIME 2. Each of the materials needed to replicate the entirety of microbiome analysis can also be found on this project's GitHub repository located at github.com/kdprkr/MerlinsManuscript. Please contact the corresponding author if any item needed for microbiome analysis or generation of figures and tables cannot be found, or if any links are broken.

Non-targeted metabolomics sample processing

The mouse diets, proximal and distal colon tissues, and whole blood samples were sent to Metabolon Inc © (Durham, NC, USA) for metabolite extraction and metabolite identifications. Mouse diets (200mg), colon tissue (50 milligrams) and whole blood (one mL) were provided on dry ice and were stored at -80^{0}C until use. Each matrix was extracted with 80% methanol and divided into five equal parts for chromatographic extraction including two rounds of reverse-phase ultra-high performance liquid chromatography tandem mass-spectrometry (UPLC-MS/MS) with positive ion mode electrospray ionisation (ESI), one round of reverse-phase UPLC-MS/MS with negative ion mode ESI, one round of hydrophilic-interaction (HILIC)/UPLC-MS/MS with negative ion mode ESI and one back-up sample. Aliquots collected under acidic conditions for positive ion mode analysis of hydrophilic compounds were separated on a C18 column (Waters UPLC BEH C18-2.1x100 mm, 1.7 µm) and gradient-eluted using a water and methanol mobile phase with 0.1% v/v formic acid. Aliquots collected under acidic conditions for positive ion mode analysis of hydrophobic compounds were separated on the same column but were gradient-eluted with a mobile phase containing water, methanol, 0.05% v/v penta-fluoropropionic anhydride and 0.01% formic acid. Aliquots collected under basic conditions for negative ion ESI were separated using a

For Peer Review

separate C18 column (Waters UPLC BEH C18-2.1x100 mm, 1.7 µm) and gradient-eluted using a water and acetonitrile mobile phase with 6.5 millimolar ammonium bicarbonate at pH of eight. The HILIC aliquot was separated using a HILIC column (Waters UPLC BEH Amide 2.1x150 mm, 1.7µm) and gradient-eluted using a water and acetonitrile mobile phase with 10 millimolar ammonium formate at pH 10.8. Each chromatographically-extracted sample was stored overnight under nitrogen gas before mass-spectral analysis, which was performed on a Thermo Scientific Q-Exactive mass spectrometer operated with a heated-ESI source and at a 35,000-mass resolution. Tandem mass spectrometry scans alternated between MS and MSn scans using dynamic exclusion and covered a range of 70 m/z (mass to charge ratio) to 1,000 m/z. Mass spectral profiles were peak identified and quality-control processed at Metabolon Inc ©. Quality control during sample processing was measured by injecting a cocktail of known chemical standards into each sample prior to chromatography and mass spectrometry, via spectral analysis of a pooled matrix sample containing an equal volume of each sample and using extracted water samples as negative controls. Compound identities were made based on an internal library containing over 3,300 commercially available chemical standards and were annotated based on matches to retention time/index, having an m/z within 10 parts per million to a database standard, and by assessing the overall mass spectral profile matches to database standards. Spectral profiles that were structurally resolved but were otherwise not archived in internal chemical database were reported as 'unknown'.

Metabolomics statistical analysis

Metabolite raw abundances were normalised by dividing the median raw abundance of that metabolite across the entire dataset for each matrix, and to produce median-scaled abundances. For samples lacking a metabolite, the minimum median scaled abundance of that metabolite across the dataset was input as a minimum value before downstream statistical analysis. Metabolite fold differences were calculated for each metabolite by dividing the average median-scaled abundance of the metabolite in one treatment group by that of a second treatment group for all pairs of treatments within a matrix. For the colon tissue, metabolite median-scaled abundances and fold differences were calculated by pooling together proximal and distal colon into a single sample type. For the study diets (food), colon tissue, and blood, median-scaled abundances for each metabolite were compared using two-way analysis of variance (ANOVA) with a Welch's post-hoc test, where significance was defined as $P<0.05$. To account for false discovery rate errors, a q-value was calculated for each metabolite and metabolites with a q-value less than 0.1 were excluded from downstream analysis.

Metabolic network visualisation

Metabolic network visualisation with Cytoscape Network Analysis version 2.8.3 was performed to compare the abundances of metabolites that were statistically-different ($P<0.05$) between *B. longum*-fermented rice bran and rice bran samples in the food, colon tissue, and blood metabolomes. Metabolites were organised into nodal clusters by chemical class (e.g. lipid, amino acid) and were further separated by metabolic pathway (e.g. sphingolipid, polyamine). Node diameters measured the magnitude of each metabolite's fold difference between *B. longum*-fermented rice bran and rice bran samples where larger node diameters reflected larger fold difference magnitudes between *B. longum*-fermented rice bran versus rice bran. Red nodes indicated metabolites that increased in *B. longum*-fermented rice bran versus rice bran and blue nodes indicated metabolites that were significantly decreased. Numbers in nodes are pathway enrichment scores (PES) that indicate a metabolic pathway's relative contribution of statistically-significant metabolites to treatment differences. Pathway enrichment scores were calculated using the following equation:

For Peer Review

$$PES = \frac{(m - k)}{(N - n)}$$

The score is determined by subtracting a pathway's number of statistically-different metabolites (k) from the total number of metabolites in the pathway (m) and then dividing this by the difference in the total number of statistically different metabolites in the entire dataset (n) and the total number of metabolites in the dataset (N). Metabolites with a PES>1.0, indicated a higher proportion of statistically-different metabolites compared to all other pathways, and thus designated pathways contributing to treatment differences.

Results

Metabolome differences between the B. longum-fermented rice bran and the rice bran diets

Metabolomics of the food identified 663 distinct metabolites that were organised by chemical class and metabolic pathway in Sheet S1. A total of 180 metabolites were statistically-different in abundances between the *B. longum*-fermented rice bran and rice bran diets including 56 amino acids (39 increased in fermented rice bran versus rice bran, 17 decreased), two peptides (two increased), eight carbohydrates (six increased, two decreased), three energy pathway metabolites (two increased, one decreased), 34 lipids (16 increased, 18 decreased), 26 nucleotides (25 increased, one decreased), nine cofactors and vitamins (three increased, six decreased), 17 phytochemicals (11 increased, six decreased), and 25 unknown metabolites (eight increased, 17 decreased). These differentially abundant metabolites are visualised for *B. longum*-fermented rice bran versus rice bran diets in Figure 2 and listed in Table S1, with reported colorectal cancer-protective and antimicrobial functions described in Table S2.

Notably, lipids and amino acids contributed to ~50% of the metabolite differences between fermented rice bran and rice bran diets with nucleotides (~14% of differences), phytochemicals (~9% of differences), and unknown/unnamed metabolites (~14% of differences). Metabolic pathways contributing to the lipids that differed between fermented rice bran and rice bran mouse diets included mevalonate (PES 3.50), glycerolipid (3.50), acyl choline (3.50), medium chain fatty acid (3.50), amino fatty acid (3.50), neurotransmitter (3.50), phosphatidylinositol (3.50), phospholipid (1.70), phosphatidylglycerol (1.70), dihydroxy fatty acid (1.70), and glycolipid (1.20) .The amino acid pathways were: glutathione (PES 2.30), alanine and aspartate (2.30), urea cycle, arginine and proline (2.30), polyamine (2.20), tyrosine (2.20), histidine (1.80), glutamate (1.70), lysine (1.30), and leucine, isoleucine and valine (1.10). Lipids and amino acids driving the metabolic pathway differences were N-delta-acetylornithine (170.87 fold-increase in fermented rice bran versus rice bran), (N(1) + N(8))-acetylspermidine (2.11 fold-increase), glutathione, oxidised (0.34 fold-decrease), and glutamine (0.72 fold-decrease) (Figure 2, Table S1, Sheet S1). Other metabolic pathways distinguishing fermented rice bran and rice bran foods were phytochemical pathways benzenes (3.50 PES), the tricarboxylic acid cycle energy pathway (1.30), and the nucleotide pathway guanine (2.00), cytidine (1.50). Metabolites contributing to these additional pathway distinctions of the foods were cytosine (50.58 fold-increase in fermented rice bran versus rice bran), 2'-deoxyguanosine (2.35 fold-increase), salicylate (1.35 fold-increase), and tricarballylate (1.24 fold-increase).

Bacterial composition of the caecum, colon, and faeces of mice fed control, rice bran, or B. longum-fermented rice bran diets

The relative abundances of any SV sharing taxonomic affiliation with the genus *Bifidobacterium* was used to determine whether an enrichment of the fermenting strain occurred in the microbiomes of mice consuming *B. longum*-fermented rice bran. A total of nine SVs had *Bifidobacterium* assignments; six were not assigned beyond the genus level,

For Peer Review

two were identified as *Bifidobacterium pseudolongum*, and 1 was assigned as *Bifidobacterium bifidum*. The three SVs with species level assignments were nearly undetectable across microbiomes of mice from all study diets and all sample types, while the six *Bifidobacterium* SVs were primarily present in faecal samples, independent of study diet (Figure S1 A-C). These results indicate minimal enrichment of the fermenting strain in the gut microbiomes of mice consuming *B. longum*-fermented rice bran.

Taxonomy-independent microbiota composition was qualitatively explored using centred log-ratio transformed SV abundances ordinated by PCA. These results revealed a separation between faecal microbiomes and microbiomes originating from the caecum and colon, with the latter sample types showing relative similarity to one another (Figure 3A). Comparisons by diet groups indicated compositional differences between control and mice fed with either rice bran or *B. longum*-fermented rice bran (Figure 3B). No clear separation or trend was observed between microbiomes from mice fed rice bran or *B. longum*-fermented rice bran (Figure 3B). Importantly, negative controls were ordinated alongside diets, and broad relationships between sample types and study diets persisted (Figure S2).

Given the similarity for both proximal and distal colon and caecum microbiomes reported above, these tissues were grouped, and differentially abundant SVs were assessed in pairwise for all diet combinations using ALDEx2. Thirty differentially abundant SVs were identified between microbiomes from mice fed a control diet or a rice bran diet; 16 higher in control and 14 higher in rice bran (Table S3). Fifty-eight differentially abundant SVs were identified between microbiomes from mice fed a control diet or a *B. longum*-fermented rice bran diet; 36 higher in control and higher in *B. longum*-fermented rice bran (Table S3). Six identical SVs showed higher proportion in both experimental diets when either was compared to control (Figure S3). The pairwise comparison between experimental diet groups resulted in 2 differentially abundant SVs. One SV was taxonomically assigned by the SILVA classifier to the genus *Roseburia* and showed higher proportion in mice fed *B. longum*-fermented rice bran (Figure 4A). The second SV's taxonomic resolution was limited to the order level, assigned as Clostridiales, and exhibited higher proportion in mice fed rice bran (Figure 4B).

B. longum-fermented rice bran diets modulate the bioavailability of compounds in the colon metabolome of healthy mice

A total of 664 metabolites were identified in the colon metabolome. The complete list was included in Sheet S1. In the colon tissue, there were 125 amino acids, 25 peptides, 33 carbohydrates, 12 energy metabolites, 301 lipids, 43 nucleotides, 34 cofactors/vitamins, 25 phytochemicals/others, and 66 unknown metabolites. Eighty metabolites significantly-differed in abundance ($P<0.05$) in the colon tissue between *B. longum*-fermented rice bran and rice bran fed mice and included three amino acids (three increased), one energy metabolite (one increased), 69 lipids (69 decreased), one nucleotide (one increased), two cofactors/vitamins (two decreased), two phytochemicals/other (one increased, one decreased), and two unknown metabolites (two increased). Figure 5 shows the lipid metabolites that comprised the majority class of significant metabolites (~86%) in the colon tissue of *B. longum*-fermented rice bran fed mice versus rice bran-fed mice (69 increased). Lipid metabolic pathways driving these diet-differences included sphingosine (PES 7.70), sphingolipid synthesis (7.70), sphingomyelin (5.80), polyunsaturated fatty acid (2.20), and sterol (1.90). Lipid metabolites contributing to metabolic pathway differences included the polyunsaturated fatty acid nisinate (0.12 fold-decrease in the colon tissue of fermented rice versus rice bran-fed mice), the sphingolipid synthesis metabolites sphinganine (0.53 fold-decrease), sphingadienine (0.45 fold decrease), the sphingomyelin metabolite palmitoyl-sphingomyelin (0.55 fold-decrease), the sphingosine metabolite sphingosine (0.57 fold-decrease), and the sterol cholesterol (0.53 fold-decrease). A complete list of the differentially

For Peer Review

abundant known metabolites was visualised for the colon tissue of *B. longum*-fermented rice bran fed mice versus rice bran fed mice in Figure 5 and are listed in Table S1, and these statistically-different colon tissue metabolites with reported colorectal cancer-protective and antimicrobial functions are described in Table S2.

B. longum-fermented rice bran diets modulate the blood metabolome of healthy mice.

A total of 802 metabolites were identified in the blood metabolome including 172 amino acids, 36 peptides, 31 carbohydrates, 11 energy metabolites, 354 lipids, 43 nucleotides, 20 cofactors/vitamins, 44 phytochemicals/others, and 91 unknown metabolites (Sheet S1). Fifty blood metabolites had significantly-different (P<0.05) abundances between mice fed fermented rice bran versus rice bran including 19 amino acids (14 increased, five decreased), three peptides (three increased), two carbohydrates (two increased), 13 lipids (nine increased, four decreased), three nucleotides (one increased, two decreased), one cofactors/vitamins (one increased), four phytochemicals/others (three increased, one decreased), and five unknown metabolites (three increased, two decreased). Lipid (26%) and amino acid (38%) metabolites accounted for the majority of blood metabolites with statistically-different (P<0.05) abundances between mice fed *B. longum*-fermented rice bran versus rice bran. Lipid and amino acid metabolic pathways contributing to these blood metabolome differences included inositol (PES 18.23), secondary bile acid (2.03), primary bile acid (1.66), glutathione (3.65), polyamine (3.04), glutamate (2.03), and urea cycle, arginine and proline (1.82). Metabolites driving differences across these pathways included the urea cycle, arginine and proline metabolite N-delta-acetyl-ornithine (4.44 fold-increased in the blood of mice consuming fermented rice bran versus rice bran), the primary bile acid chenodeoxycholate (1.79 fold-increase), the secondary bile acid deoxycholate (1.49 fold-increase), the polyamine 5-methylthioadenosine (1.54 fold-increase), the glutathione metabolite glutathione, oxidised (1.53 fold-increase), the glutamate metabolite glutamine (1.31 fold-increase), the polyunsaturated fatty acid arachidonate (1.28 fold-increase), and the inositol metabolite myo-inositol (0.67 fold-decrease). The statistically-different blood metabolites between diet groups are provided in Table 2 and Table S1, and those with reported colorectal cancer-protective and antimicrobial functions are described in Table S2.

Table 2. Differentially abundant blood metabolites in mice consuming *B. longum*-fermented rice bran versus rice bran diets.

Metabolic Pathway (PES)[1]	Metabolites	Fold Difference[2] FRB / RB	*P*-value
Amino Acids			
Alanine and Aspartate (2.60)	N-acetylasparagine	↑1.33	0.043
Glutamate (2.03)	glutamine	↑1.31	0.044
Histidine (1.07)	1-methyl-4-imidazole acetate	↑1.26	0.0085
Tryptophan (1.07)	N-formylanthranilic acid	↑1.25	0.014
Lysine (1.82)	2-oxoadipate	↓0.69	0.026
Tyrosine (2.80)	tyrosine	↑1.32	0.043
	1-carboxyethyltyrosine	↑1.49	0.030
Leucine, Isoleucine and Valine (0.63)	3-methylglutaconate	↑1.32	0.027
Methionine, Cysteine, and Taurine (1.22)	N-formylmethionine	↑1.24	0.0093
Urea Cycle, Arginine and Proline (1.82)	N-delta-acetylornithine	↑4.44	0.0052
	N2,N5-diacetylornithine	↑2.09	7.33E-8
Polyamine (3.04)	5-methylthioadenosine	↑1.54	0.022
Glutathione (3.65)	glutathione, oxidised	↑1.53	0.035
	ophthalmate	↑1.39	0.049
Peptides			
Dipeptide (3.65)	valylglycine	↑2.87	0.0096
Carbohydrates			
Pentose (4.05)	arabitol/xylitol	↑1.48	0.0068
	arabonate/xylonate	↑1.12	0.037
Lipids			

For Peer Review

Carnitine (1.07)	propionylcarnitine	↑1.53	0.033
	cis-4-decenoylcarnitine	↑1.59	0.047
Polyunsaturated Fatty Acid (1.01)	arachidonate	↑1.28	0.033
Dicarboxylate Fatty Acid (1.07)	octadecenedioate*	↑1.36	0.031
Inositol (18.23)	myo-inositol	↓0.67	0.020
Phopspholipid (2.28)	choline	↑1.30	0.0076
Plasmalogen (2.28)	1-(1-enyl-palmitoyl)-2-linoleoyl-glycerophosphocholine	↓0.78	0.033
Diacylglycerol (1.01)	oleoyl-oleoyl-glycerol*	↓0.36	0.045
Lactosylceramides (18.23)	lactosyl-N-palmitoyl-sphingosine	↓0.40	0.023
Primary Bile Acid (1.66)	chenodeoxycholate	↑1.79	0.033
Secondary Bile Acid (2.03)	deoxycholate	↑1.49	0.0062
Nucleotides			
Uracil (1.40)	N-acetyl-beta-alanine	↓0.20	0.00050
Cytidine (3.04)	cytosine	↑5.67	0.00040
Thymine (6.08)	5,6-dihydrothymine	↓0.31	0.022
Vitamins/Cofactors			
Tetrahydrobiopterin (9.12)	biopterin	↑1.19	0.044
Hemoglobin and Porphyrin (6.08)	biliverdin	↑2.10	0.047
Phytochemical/Other			
Phytochemical (1.52)	2-hydroxyhippurate (salicylurate)	↑2.27	0.023
	thioproline	↓0.77	0.0030
Other (2.14)	ergothionine	↑1.77	0.0072
	erythritol	↑1.32	0.017

1. PES: Pathway enrichment score
2. FRB: Fermented Rice Bran; RB: Rice Bran
* Indicates metabolite annotation was not made via an internal Metabolon library standard but predicted using spectral profiles from curated chemical databases.

Discussion

We examined daily dietary intake of *B. longum*-fermented rice bran for metabolic distinctions to non-fermented rice bran or a control diet intake for 15 weeks in healthy mice. Dietary interventions were assessed for effects on gut microbial bacterial community composition and for uptake of metabolic by-products into the host in the colon tissue and blood. This study showed that despite considerable differences in the food metabolomes of *B. longum*-fermented rice bran and non-fermented rice bran, the effects were subtle on the gut microbiota composition. Using a healthy murine model was a key aspect of these investigations as colon microbiome composition, and blood and colon metabolite profiles were not disturbed, and thus the differences in the colon tissue and blood metabolomes detected between mice fed *B. longum*-fermented rice bran versus the non-fermented form have strong implications for mechanisms involved in enteric disease prevention.

Compositional analysis of caecum and colon microbiomes indicated clear differences between mice fed a control diet and mice fed with either rice bran or *B. longum*-fermented rice bran; however, the differences between experimental diets were limited. The sequencing methodologies employed in this study did not differentiate between metabolically active, dormant, or dead prokaryotic organisms (Emerson *et al.*, 2017). The low abundance of *Bifibacterium* spp. in caecum and colon microbiomes and the similar abundance in faecal microbiomes across all study diets indicated nominal, if any, enrichment of the fermenting strain in microbiomes of mice consuming *B. longum*-fermented rice bran. The two SV's identified as differentially abundant did taxonomically affiliate with the genus *Roseburia* and was associated with mice fed a *B. longum*-fermented rice bran diet. This was of particular interest because *Roseburia* are known to produce beneficial short-chain fatty acids, in addition to other compounds exerting anti-inflammatory activity in the gut (Tamanai-Shacoori *et al.*, 2017). Reduced abundance or loss of *Roseburia* spp. have been associated with a variety of diseases, including colorectal cancer (Rezasoltani *et al.*, 2018). An additional differentially abundant SV represented by *Roseburia* was identified for paired comparisons of each experimental diet to control and showed strong association with rice bran and *B. longum*-fermented rice bran fed mice.

For Peer Review

The *B. longum*-fermented rice bran and rice bran diets exhibited large differences in host uptake and metabolism of bioactive molecules in the colon and blood that had previously reported colorectal cancer-protective and antimicrobial functions. The lipid and amino acid metabolic pathways represented the majority of metabolite abundance changes in the food, colon tissue, and blood metabolomes when with *B. longum*-fermented rice bran fed mice were compared to rice bran fed mice. Increased bioavailability of N-delta-acetylornithine in colon (11.77-fold increase) and blood (4.44-fold increase) when comparing mice consuming fermented rice bran versus rice bran was supported by substantially increased abundance in the food (170.87-fold increase). N-delta-acetylornithine is a secondary metabolite of plants that has roles in protecting plant tissues from herbivore damage and bacterial infections (Adio *et al.*, 2011). Previous studies have shown that some colorectal cancer tumours had lower levels of N-delta-acetylornithine when compared to levels in health mucosal colonocytes (Gómez de Cedrón *et al.*, 2017), suggesting that depletion of this metabolite may either promote or facilitate the dysregulated metabolism associated with colorectal cancer pathogenesis. The increased colon and blood levels of N-delta-acetylornithine merit mechanistic examination for its effects on host colonocyte metabolism.

Another potential regulator of colonocyte and gut bacterial metabolism was demonstrated by the increased uptake of tricarballylate (23.34 fold-increase) in mice consuming *B. longum*-fermented rice bran compared to rice bran alone. Tricarballylate has been previously reported to function as an aconitase inhibitor where it decreased the conversion of citrate into isocitrate to reduce metabolite flux through the tricarboxylic acid cycle and diminished *Salmonella* proliferation (Nealon *et al.*, 2017; Watson *et al.*, 1969). When tricarballylate was administered to rats, decreased succinate was produced in colonocytes, which is a downstream product of citrate metabolism in the tricarboxylic acid cycle, suggesting that its biochemical mechanisms also function in mammalian systems (Wolffram *et al.*, 1994). Tricarballylate-mediated interference in colorectal cancer cell function has not been characterised; however, given the increased tricarboxylic acid cycle activity reported in multiple cancer types and in several lines of chemotherapy-resistant neoplastic colonocytes (Zhou *et al.*, 2012), tricarballylate from foods or foods that increase tricarballylate uptake by colonocytes warrant investigation for possible protection against colorectal cancer. Also noteworthy was that a decreased pH in the lumen enhanced tricarballylate uptake into colonocytes (Zhou *et al.*, 2012). Given the capacity of rice bran to be fermented in the colon lumen, it is plausible to suggest that *B. longum*-fermented rice bran increased the availability of fermentable substrates to the murine colon microbiota thereby creating a lower pH-environment to favour enhanced tricarballylate uptake when compared to mice consuming the non-fermented rice bran diet.

While the *B. longum*-fermented rice bran diet metabolome itself delivered different levels of bioactive metabolites to the host compared to the rice bran diet, differential metabolism of fermented rice bran versus rice bran within the host further influenced levels of enteric disease protective metabolites. For example, the bile acid 4-cholesten-3-one was not differentially abundant between the *B. longum*-fermented and rice bran diets, but it was significantly lowered in the colon tissue (0.74-fold decrease) of mice consuming fermented rice bran compared to mice consuming rice bran alone. In colon tissue, 4-cholesten-3-one has been shown to increase inflammatory responses by the mucosal immune system via decreasing the production of the anti-inflammatory cytokine tumour growth factor beta, and it was significantly-increased in the faeces of adults with colorectal cancer versus healthy adults (Chen *et al.*, 2017a). Decreased 4-cholensten-3-one in the colon tissue of mice consuming *B. longum*-fermented rice bran may suggest that fermented rice bran exerts cancer-protective effects by modulating host colonocyte metabolism when compared to rice bran alone. Chronic inflammation facilitates both tumour initiation and promotion in colorectal cancer (Chen *et*

For Peer Review

al., 2017b), and this investigation of fermented foods that reduce inflammatory cascades could contribute guidelines for disease prevention.

Conclusions

B. longum-fermented rice bran did not considerably modulate the healthy murine faecal, caeca, or colon microbiomes when compared to non-fermented rice bran, yet the diet did elicit production of a suite of unique food and microbial metabolites that were identified in the host colon and bloodstream. Most of these changes were amino acids and lipids produced by both the host and the gut microbiome that have important implications for detailed assessments of fermented diets and for enhancing bioavailability and promoting colon health. The assessment of metabolome and microbiome in concert provided an important and powerful approach to further our understanding of how fermentation modulates bioactivity of rice bran in a healthy host system. This study design and methodology has utility for screening of probiotic strains that will optimise rice bran's capacity for safety, prophylaxis and therapeutic potential aimed toward gastrointestinal disorders across the lifespan.

Acknowledgements

The authors thank Renee C. Oppel for technical assistance and preparation of the *B. longum*-fermented rice bran diet. Funding for this study was provided by the National Institutes of Health-National Cancer Institute (1R01CA201112-02) as a multi-investigator award of E. P. Ryan and K. Raina. Lastly, we wish to thank all of the mice sacrificed in the work presented here for their contributions towards the pursuit of understanding.

Figure Legends

Figure 1. Study design and timeline of sampling.
Male BALB/c mice were fed control, rice bran, or *B. longum*-fermented rice bran diets for 15 weeks. Faeces, caecum, and colon were collected for both microbiota and metabolite analysis; blood was collected for metabolite analysis only.

Figure 2. Fermentation with *B. longum* alters the rice bran food metabolome.
Metabolites that were statistically-different in abundance between *B. longum*-fermented rice bran and rice bran food metabolomes are depicted. Metabolites are organised by chemical class and further stratified by metabolic pathway, where each coloured node represents one metabolite. Node diameter reflects the magnitude of the fold abundance difference for the metabolite between *B. longum*-fermented rice bran and rice bran. Red nodes indicate metabolites that were significantly-increased in *B. longum*-fermented rice bran versus rice bran, and blue nodes indicate metabolites that were significantly-decreased in *B. longum*-fermented rice bran versus rice bran. Numbers in nodes are pathway enrichment scores.

Figure 3. Healthy murine microbiomes exhibit clear separation in community composition based upon sample type and diet group.
Principal components analysis of centred log-ratio transformed absolute abundances for all sequence variants with abundance greater than two in faecal, colon, and caecum samples. Percentage values along each axis indicate the amount of variation explained by each of the first two principal components. [A] Symbols and colours denote sample type (faecal, caecum, distal or proximal colon; see key). [B] Letters and s denote mouse diet group (control, rice bran, *B. longum*-fermented rice bran; see key).

For Peer Review

Figure 4. Consumption of *B. longum*-fermented rice bran versus rice bran minimally alters the caecum and colon microbiomes of healthy mice.
[A-B] Strip charts of median centred log-ratio values for two sequence variants considered to be differentially abundant (q<0.1) between microbiomes from mice fed a *B. longum*-fermented rice bran or a rice bran diet. Symbols denote sample type (caecum, distal or proximal colon; see key); line style and colours denote mouse diet (rice bran, *B. longum*-fermented rice bran; see key). Lines represent the median clr value for all samples within a diet group, while points represent the median clr value for each individual sample. Sequence variant taxonomic identities from Greengenes and SILVA databases are indicated on the x-axis styled as Greengenes/SILVA.

Figure 5. Consumption of *B. longum*-fermented rice bran versus rice bran alters the colon tissue metabolome of healthy mice.
Metabolites that were statistically-different in abundance between *B. longum*-fermented rice bran versus rice bran-fed mice are depicted. Metabolites are organised by chemical class and further stratified by metabolic pathway, where each coloured node represents one metabolite. Node diameter reflects the magnitude of the fold abundance difference for the metabolite between *B. longum*-fermented rice bran and rice bran. Red nodes indicate metabolites that were significantly-increased in the colon of *B. longum*-fermented rice bran fed mice versus rice bran fed mice, and blue nodes indicate metabolites that were significantly-decreased in *B. longum*-fermented rice bran versus rice bran. Numbers in nodes are pathway enrichment scores.

Figure S1. Consumption of *B. longum*-fermented rice bran versus rice bran or control does not enrich the fermenting strain
Stacked bar charts of relative abundance data from nine sequence variants assigned to the genus *Bifidobacterium*. Taxonomic assignment was made to the lowest possible taxonomic level that could be achieved with confidence threshold equal to or above 0.75 for both Greengenes- and SILVA-based classifiers. Panels are grouped by study diet [A-C] or negative controls [D].

Figure S2. Experimental microbiome samples display dissimilarity from negative control samples.
Principal components analysis of centred log-ratio transformed absolute abundances for all sequence variants with abundance greater than two in faecal, colon, and caecum experimental samples alongside negative controls. Percentage values along each axis indicate the amount of variation explained by each of the first two principal components. [A] Symbols and colours denote sample type (see key). [B] Letters and colours denote mouse diet (see key).

Figure S3. Consumption of a rice bran or *B. longum*-fermented rice bran diet alters healthy murine microbiome composition.
[A-F] Strip charts of median centred log-ratio values for six differentially abundant (q<0.1) sequence variants exhibiting conserved enrichment in microbiomes from mice fed rice bran or *B. longum*-fermented rice bran diets compared to mice fed a control diet. Symbols denote sample type; line style and colours denote mouse diet (see key). Lines represent the median clr value for all samples within a diet group, while points represent the median clr value for each individual sample. Sequence variant taxonomic identities from Greengenes and SILVA databases are indicated on the x-axis as Greengenes/SILVA.

For Peer Review

References

Adio, A.M., Casteel, C.L., De Vos, M., Kim, J.H., Joshi, V., Li, B., Juery, C., Daron, J., Kliebenstein, D.J. and Jander, G., 2011. Biosynthesis and defensive function of Ndelta-acetylornithine, a jasmonate-induced Arabidopsis metabolite. Plant Cell 23: 3303-3318. 10.1105/tpc.111.088989

Ahn, E.H. and Schroeder, J.J., 2006. Sphinganine causes early activation of JNK and p38 MAPK and inhibition of AKT activation in HT-29 human colon cancer cells. Anticancer Res 26: 121-127.

Ahn, E.H. and Schroeder, J.J., 2010. Induction of apoptosis by sphingosine, sphinganine, and C(2)-ceramide in human colon cancer cells, but not by C(2)-dihydroceramide. Anticancer Res 30: 2881-2884.

Bazanella, M., Maier, T.V., Clavel, T., Lagkouvardos, I., Lucio, M., Maldonado-Gomez, M.X., Autran, C., Walter, J., Bode, L., Schmitt-Kopplin, P. and Haller, D., 2017. Randomized controlled trial on the impact of early-life intervention with bifidobacteria on the healthy infant fecal microbiota and metabolome. Am J Clin Nutr 106: 1274-1286. 10.3945/ajcn.117.157529

Becker, J.C., Fukui, H., Imai, Y., Sekikawa, A., Kimura, T., Yamagishi, H., Yoshitake, N., Pohle, T., Domschke, W. and Fujimori, T., 2007. Colonic expression of heme oxygenase-1 is associated with a better long-term survival in patients with colorectal cancer. Scand J Gastroenterol 42: 852-858. 10.1080/00365520701192383

Bibel, D.J., Aly, R. and Shinefield, H.R., 1992. Inhibition of microbial adherence by sphinganine. Can J Microbiol 38: 983-985.

Bou Ghanem, E.N., Lee, J.N., Joma, B.H., Meydani, S.N., Leong, J.M. and Panda, A., 2017. The Alpha-Tocopherol Form of Vitamin E Boosts Elastase Activity of Human PMNs and Their Ability to Kill Streptococcus pneumoniae. Front Cell Infect Microbiol 7: 161. 10.3389/fcimb.2017.00161

Bradford, E.M., Thompson, C.A., Goretsky, T., Yang, G.Y., Rodriguez, L.M., Li, L. and Barrett, T.A., 2017. Myo-inositol reduces beta-catenin activation in colitis. World J Gastroenterol 23: 5115-5126. 10.3748/wjg.v23.i28.5115

Bokulich, N.A., Kaehler, B.D., Rideout, J.R., Dillon, M., Bolyen, E., Knight, R., Huttley, G.A. and Gregory Caporaso, J., 2018. Optimizing taxonomic classification of marker-gene amplicon sequences with QIIME 2's q2-feature-classifier plugin. Microbiome 6: 90. 10.1186/s40168-018-0470-z

Brown, D.G., Borresen, E.C., Brown, R.J. and Ryan, E.P., 2017. Heat-stabilised rice bran consumption by colorectal cancer survivors modulates stool metabolite profiles and metabolic networks: a randomised controlled trial. Br J Nutr 117: 1244-1256. 10.1017/s0007114517001106

Bunesova, V., Lacroix, C. and Schwab, C., 2016. Fucosyllactose and L-fucose utilization of infant Bifidobacterium longum and Bifidobacterium kashiwanohense. BMC Microbiol 16: 248-248. 10.1186/s12866-016-0867-4

Callahan, B.J., McMurdie, P.J., Rosen, M.J., Han, A.W., Johnson, A.J. and Holmes, S.P., 2016. DADA2: High-resolution sample inference from Illumina amplicon data. Nat Methods 13: 581-583. 10.1038/nmeth.3869

Caporaso, J.G., Kuczynski, J., Stombaugh, J., Bittinger, K., Bushman, F.D., Costello, E.K., Fierer, N., Peña, A.G., Goodrich, J.K., Gordon, J.I., Huttley, G.A., Kelley, S.T., Knights, D., Koenig, J.E., Ley, R.E., Lozupone, C.A., McDonald, D., Muegge, B.D., Pirrung, M., Reeder, J., Sevinsky, J.R., Turnbaugh, P.J., Walters, W.A., Widmann, J., Yatsunenko, T., Zaneveld, J. and Knight, R., 2010. QIIME allows analysis of high-throughput community sequencing data. Nature methods 7: 335-336. 10.1038/nmeth.f.303

For Peer Review

Caporaso, J.G., Lauber, C.L., Walters, W.A., Berg-Lyons, D., Huntley, J., Fierer, N., Owens, S.M., Betley, J., Fraser, L., Bauer, M., Gormley, N., Gilbert, J.A., Smith, G. and Knight, R., 2012. Ultra-high-throughput microbial community analysis on the Illumina HiSeq and MiSeq platforms. The Isme Journal 6: 1621. 10.1038/ismej.2012.8 https://www.nature.com/articles/ismej20128#supplementary-information

Caporaso, J.G., Lauber, C.L., Walters, W.A., Berg-Lyons, D., Lozupone, C.A., Turnbaugh, P.J., Fierer, N. and Knight, R., 2011. Global patterns of 16S rRNA diversity at a depth of millions of sequences per sample. Proceedings of the National Academy of Sciences 108: 4516. 10.1073/pnas.1000080107

Celiberto, L.S., Bedani, R., Dejani, N.N., Ivo de Medeiros, A., Sampaio Zuanon, J.A., Spolidorio, L.C., Tallarico Adorno, M.A., Amancio Varesche, M.B., Carrilho Galvao, F., Valentini, S.R., Font de Valdez, G., Rossi, E.A. and Cavallini, D.C.U., 2017. Effect of a probiotic beverage consumption (Enterococcus faecium CRL 183 and Bifidobacterium longum ATCC 15707) in rats with chemically induced colitis. PLoS One 12: e0175935. 10.1371/journal.pone.0175935

Chemsa, A.E., Zellagui, A., Ozturk, M., Erol, E., Ceylan, O., Duru, M.E. and Lahouel, M., 2018. Chemical composition, antioxidant, anticholinesterase, antimicrobial and antibiofilm activities of essential oil and methanolic extract of Anthemis stiparum subsp. sabulicola (Pomel) Oberpr. Microb Pathog 119: 233-240. 10.1016/j.micpath.2018.04.033

Chen, C.L., Wu, D.C., Liu, M.Y., Lin, M.W., Huang, H.T., Huang, Y.B., Chen, L.C., Chen, Y.Y., Chen, J.J., Yang, P.H., Kao, Y.C. and Chen, P.Y., 2017a. Cholest-4-en-3-one attenuates TGF-beta responsiveness by inducing TGF-beta receptors degradation in Mv1Lu cells and colorectal adenocarcinoma cells. J Recept Signal Transduct Res 37: 189-199. 10.1080/10799893.2016.1203944

Chien, R.C., Lin, Y.C. and Mau, J.L., 2017. Apoptotic Effect of Taiwanofungus salmoneus (Agaricomycetes) Mycelia and Solid-State Fermented Products on Cancer Cells. Int J Med Mushrooms 19: 777-495. 10.1615/IntJMedMushrooms.2017024264

Chen, J., Pitmon, E. and Wang, K., 2017b. Microbiome, inflammation and colorectal cancer. Semin Immunol 32: 43-53. 10.1016/j.smim.2017.09.006

Cowan, T.E., Palmnas, M.S., Yang, J., Bomhof, M.R., Ardell, K.L., Reimer, R.A., Vogel, H.J. and Shearer, J., 2014. Chronic coffee consumption in the diet-induced obese rat: impact on gut microbiota and serum metabolomics. J Nutr Biochem 25: 489-495. 10.1016/j.jnutbio.2013.12.009

Deng, H. and Fang, Y., 2012. Aspirin metabolites are GPR35 agonists. Naunyn Schmiedebergs Arch Pharmacol 385: 729-737. 10.1007/s00210-012-0752-0

Derkach, A., Sampson, J., Joseph, J., Playdon, M.C. and Stolzenberg-Solomon, R.Z., 2017. Effects of dietary sodium on metabolites: the Dietary Approaches to Stop Hypertension (DASH)-Sodium Feeding Study. Am J Clin Nutr 106: 1131-1141. 10.3945/ajcn.116.150136

DeSantis, T.Z., Hugenholtz, P., Larsen, N., Rojas, M., Brodie, E.L., Keller, K., Huber, T., Dalevi, D., Hu, P. and Andersen, G.L., 2006. Greengenes, a chimera-checked 16S rRNA gene database and workbench compatible with ARB. Appl Environ Microbiol 72: 5069-5072. 10.1128/aem.03006-05

Dziaman, T., Gackowski, D., Guz, J., Linowiecka, K., Bodnar, M., Starczak, M., Zarakowska, E., Modrzejewska, M., Szpila, A., Szpotan, J., Gawronski, M., Labejszo, A., Liebert, A., Banaszkiewicz, Z., Klopocka, M., Foksinski, M., Marszalek, A. and Olinski, R., 2018. Characteristic profiles of DNA epigenetic modifications in colon cancer and its predisposing conditions-benign adenomas and inflammatory bowel disease. Clin Epigenetics 10: 72. 10.1186/s13148-018-0505-0

Emerson, J.B., Adams, R.I., Roman, C.M.B., Brooks, B., Coil, D.A., Dahlhausen, K., Ganz, H.H., Hartmann, E.M., Hsu, T., Justice, N.B., Paulino-Lima, I.G., Luongo, J.C.,

For Peer Review

Lymperopoulou, D.S., Gomez-Silvan, C., Rothschild-Mancinelli, B., Balk, M., Huttenhower, C., Nocker, A., Vaishampayan, P. and Rothschild, L.J., 2017. Schrodinger's microbes: Tools for distinguishing the living from the dead in microbial ecosystems. Microbiome 5: 86. 10.1186/s40168-017-0285-3

Fabian, C. and Ju, Y.H., 2011. A review on rice bran protein: its properties and extraction methods. Crit Rev Food Sci Nutr 51: 816-827. 10.1080/10408398.2010.482678

Fernandes, A.D., Macklaim, J.M., Linn, T.G., Reid, G. and Gloor, G.B., 2013. ANOVA-like differential expression (ALDEx) analysis for mixed population RNA-Seq. PLoS One 8: e67019-e67019. 10.1371/journal.pone.0067019

Fernandes, A.D., Reid, J.N., Macklaim, J.M., McMurrough, T.A., Edgell, D.R. and Gloor, G.B., 2014. Unifying the analysis of high-throughput sequencing datasets: characterizing RNA-seq, 16S rRNA gene sequencing and selective growth experiments by compositional data analysis. Microbiome 2: 15. 10.1186/2049-2618-2-15

Fischer, C.L., Walters, K.S., Drake, D.R., Blanchette, D.R., Dawson, D.V., Brogden, K.A. and Wertz, P.W., 2013. Sphingoid Bases Are Taken Up by Escherichia coli and Staphylococcus aureus and Induce Ultrastructural Damage. Skin Pharmacology and Physiology 26: 36-44. 10.1159/000343175

Fix, J.A., Engle, K., Porter, P.A., Leppert, P.S., Selk, S.J., Gardner, C.R. and Alexander, J., 1986. Acylcarnitines: drug absorption-enhancing agents in the gastrointestinal tract. Am J Physiol 251: G332-340. 10.1152/ajpgi.1986.251.3.G332

Forster, G.M., Raina, K., Kumar, A., Kumar, S., Agarwal, R., Chen, M.H., Bauer, J.E., McClung, A.M. and Ryan, E.P., 2013. Rice varietal differences in bioactive bran components for inhibition of colorectal cancer cell growth. Food Chem 141: 1545-1552. 10.1016/j.foodchem.2013.04.020

Gagnon, M., Savard, P., Rivière, A., LaPointe, G. and Roy, D., 2015. Bioaccessible antioxidants in milk fermented by Bifidobacterium longum subsp. longum strains. BioMed research international 2015: 169381-169381. 10.1155/2015/169381

Gentleman, R.C., Carey, V.J., Bates, D.M., Bolstad, B., Dettling, M., Dudoit, S., Ellis, B., Gautier, L., Ge, Y., Gentry, J., Hornik, K., Hothorn, T., Huber, W., Iacus, S., Irizarry, R., Leisch, F., Li, C., Maechler, M., Rossini, A.J., Sawitzki, G., Smith, C., Smyth, G., Tierney, L., Yang, J.Y. and Zhang, J., 2004. Bioconductor: open software development for computational biology and bioinformatics. Genome Biol 5: R80. 10.1186/gb-2004-5-10-r80

Glockner, F.O., Yilmaz, P., Quast, C., Gerken, J., Beccati, A., Ciuprina, A., Bruns, G., Yarza, P., Peplies, J., Westram, R. and Ludwig, W., 2017. 25 years of serving the community with ribosomal RNA gene reference databases and tools. J Biotechnol 261: 169-176. 10.1016/j.jbiotec.2017.06.1198

Gloor, G., Macklaim, J., Pawlowsky-Glahn, V. and Egozcue, J.J., 2017. Microbiome Datasets Are Compositional: And This Is Not Optional, 8, 2224 pp. 10.3389/fmicb.2017.02224

Goedert, J.J., Sampson, J.N., Moore, S.C., Xiao, Q., Xiong, X., Hayes, R.B., Ahn, J., Shi, J. and Sinha, R., 2014. Fecal metabolomics: assay performance and association with colorectal cancer. Carcinogenesis 35: 2089-2096. 10.1093/carcin/bgu131

Gómez de Cedrón, M., Acín Pérez, R., Sánchez-Martínez, R., Molina, S., Herranz, J., Feliu, J., Reglero, G., Enríquez, J.A. and Ramírez de Molina, A., 2017. MicroRNA-661 modulates redox and metabolic homeostasis in colon cancer. Molecular oncology 11: 1768-1787. 10.1002/1878-0261.12142

Greg Caporaso, M.D., Evan Bolyen, Jorden Kreps, Jai Ram Rideout, Max von Hippel, Chris Keefe, Massoud Maher, q2-demux. Available at: https://github.com/qiime2/q2-demux.

H.B. Mann, D.R.W., 1947. On a Test of Whether one of Two Random Variables is Stochastically Larger than the Other. The Annals of Mathematical Statistics 18: 50-60. 10.1214/aoms/1177730491

For Peer Review

Guo, C., Ding, P., Xie, C., Ye, C., Ye, M., Pan, C., Cao, X., Zhang, S. and Zheng, S., 2017. Potential application of the oxidative nucleic acid damage biomarkers in detection of diseases. Oncotarget 8: 75767-75777. 10.18632/oncotarget.20801

Hadley Wickham, R.F., Lionel Henry, Kirill Müller,, 2018. dplyr: A Grammar of Data Manipulation.

Han, B., Kaur, V.I., Baruah, K., Nguyen, V.D. and Bossier, P., 2019. High doses of sodium ascorbate act as a prooxidant and protect gnotobiotic brine shrimp larvae (Artemia franciscana) against Vibrio harveyi infection coinciding with heat shock protein 70 activation. Dev Comp Immunol 92: 69-76. 10.1016/j.dci.2018.11.007

Harrower, M. and Brewer, C., 2003. ColorBrewer.org: An Online Tool for Selecting Colour Schemes for Maps. The Cartographic Journal 40: 27-37. 10.1179/000870403235002042

Henderson, A.J., Kumar, A., Barnett, B., Dow, S.W. and Ryan, E.P., 2012a. Consumption of rice bran increases mucosal immunoglobulin A concentrations and numbers of intestinal Lactobacillus spp. J Med Food 15: 469-475. 10.1089/jmf.2011.0213

Henderson, A.J., Ollila, C.A., Kumar, A., Borresen, E.C., Raina, K., Agarwal, R. and Ryan, E.P., 2012b. Chemopreventive properties of dietary rice bran: current status and future prospects. Adv Nutr 3: 643-653. 10.3945/an.112.002303

Hernandez-Alonso, P., Canueto, D., Giardina, S., Salas-Salvado, J., Canellas, N., Correig, X. and Bullo, M., 2017. Effect of pistachio consumption on the modulation of urinary gut microbiota-related metabolites in prediabetic subjects. J Nutr Biochem 45: 48-53. 10.1016/j.jnutbio.2017.04.002

Hu, M., Liu, L. and Yao, W., 2018. Activation of p53 by costunolide blocks glutaminolysis and inhibits proliferation in human colorectal cancer cells. Gene 678: 261-269. 10.1016/j.gene.2018.08.048

Huber, W., Carey, V.J., Gentleman, R., Anders, S., Carlson, M., Carvalho, B.S., Bravo, H.C., Davis, S., Gatto, L., Girke, T., Gottardo, R., Hahne, F., Hansen, K.D., Irizarry, R.A., Lawrence, M., Love, M.I., MacDonald, J., Obenchain, V., Oles, A.K., Pages, H., Reyes, A., Shannon, P., Smyth, G.K., Tenenbaum, D., Waldron, L. and Morgan, M., 2015. Orchestrating high-throughput genomic analysis with Bioconductor. Nat Methods 12: 115-121. 10.1038/nmeth.3252

Kassambara, A., 2018. ggpubr: 'ggplot2' Based Publication Ready Plots.

Kim, J.H., Lee, K.J., Seo, Y., Kwon, J.H., Yoon, J.P., Kang, J.Y., Lee, H.J., Park, S.J., Hong, S.P., Cheon, J.H., Kim, W.H. and Il Kim, T., 2018. Effects of metformin on colorectal cancer stem cells depend on alterations in glutamine metabolism. Sci Rep 8: 409. 10.1038/s41598-017-18762-4

Kim, J.M., Ku, S., Kim, Y.S., Lee, H.H., Jin, H., Kang, S., Li, R., Johnston, V.T., Park, S.M. and Ji, E.G., 2018. Safety Evaluations of Bifidobacterium bifidum BGN4 and Bifidobacterium longum BORI. Int J Mol Sci 19. 10.3390/ijms19051422

Kumar, A., Henderson, A., Forster, G.M., Goodyear, A.W., Weir, T.L., Leach, J.E., Dow, S.W. and Ryan, E.P., 2012. Dietary rice bran promotes resistance to Salmonella enterica serovar Typhimurium colonization in mice. BMC Microbiol 12: 71. 10.1186/1471-2180-12-71

Law, B.M.H., Waye, M.M.Y., So, W.K.W. and Chair, S.Y., 2017. Hypotheses on the Potential of Rice Bran Intake to Prevent Gastrointestinal Cancer through the Modulation of Oxidative Stress. Int J Mol Sci 18. 10.3390/ijms18071352

Lee, T., Clavel, T., Smirnov, K., Schmidt, A., Lagkouvardos, I., Walker, A., Lucio, M., Michalke, B., Schmitt-Kopplin, P., Fedorak, R. and Haller, D., 2017. Oral versus intravenous iron replacement therapy distinctly alters the gut microbiota and metabolome in patients with IBD. Gut 66: 863-871. 10.1136/gutjnl-2015-309940

For Peer Review

Lei, S., Ramesh, A., Twitchell, E., Wen, K., Bui, T., Weiss, M., Yang, X., Kocher, J., Li, G., Giri-Rachman, E., Trang, N.V., Jiang, X., Ryan, E.P. and Yuan, L., 2016. High Protective Efficacy of Probiotics and Rice Bran against Human Norovirus Infection and Diarrhea in Gnotobiotic Pigs. Front Microbiol 7: 1699. 10.3389/fmicb.2016.01699

Li, S.A., Jiang, W.D., Feng, L., Liu, Y., Wu, P., Jiang, J., Kuang, S.Y., Tang, L., Tang, W.N., Zhang, Y.A., Yang, J., Tang, X., Shi, H.Q. and Zhou, X.Q., 2018. Dietary myo-inositol deficiency decreased intestinal immune function related to NF-kappaB and TOR signaling in the intestine of young grass carp (Ctenopharyngodon idella). Fish Shellfish Immunol 76: 333-346. 10.1016/j.fsi.2018.03.017

Li, T.W., Peng, H., Yang, H., Kurniawidjaja, S., Panthaki, P., Zheng, Y., Mato, J.M. and Lu, S.C., 2015. S-Adenosylmethionine and methylthioadenosine inhibit beta-catenin signaling by multiple mechanisms in liver and colon cancer. Mol Pharmacol 87: 77-86. 10.1124/mol.114.095679

Liu, G., Ren, W., Fang, J., Hu, C.A., Guan, G., Al-Dhabi, N.A., Yin, J., Duraipandiyan, V., Chen, S., Peng, Y. and Yin, Y., 2017. L-Glutamine and L-arginine protect against enterotoxigenic Escherichia coli infection via intestinal innate immunity in mice. Amino Acids 49: 1945-1954. 10.1007/s00726-017-2410-9

Liu, J., Xiao, H.T., Wang, H.S., Mu, H.X., Zhao, L., Du, J., Yang, D., Wang, D., Bian, Z.X. and Lin, S.H., 2016. Halofuginone reduces the inflammatory responses of DSS-induced colitis through metabolic reprogramming. Mol Biosyst 12: 2296-2303. 10.1039/c6mb00154h

Martín-Fernández, J., Hron, K., Templ, M., Filzmoser, P. and Palarea-Albaladejo, J., 2014. Bayesian-multiplicative treatment of count zeros in compositional data sets, 15. 10.1177/1471082X14535524

Martin, M., 2011. CUTADAPT removes adapter sequences from high-throughput sequencing reads, 17. 10.14806/ej.17.1.200

McDonald, D., Clemente, J.C., Kuczynski, J., Rideout, J.R., Stombaugh, J., Wendel, D., Wilke, A., Huse, S., Hufnagle, J., Meyer, F., Knight, R. and Caporaso, J.G., 2012a. The Biological Observation Matrix (BIOM) format or: how I learned to stop worrying and love the ome-ome. GigaScience 1: 2047-2217X-2041-2047-2047-2217X-2041-2047. 10.1186/2047-217X-1-7

McDonald, D., Price, M.N., Goodrich, J., Nawrocki, E.P., DeSantis, T.Z., Probst, A., Andersen, G.L., Knight, R. and Hugenholtz, P., 2012b. An improved Greengenes taxonomy with explicit ranks for ecological and evolutionary analyses of bacteria and archaea. Isme j 6: 610-618. 10.1038/ismej.2011.139

McIntosh, K., Reed, D.E., Schneider, T., Dang, F., Keshteli, A.H., De Palma, G., Madsen, K., Bercik, P. and Vanner, S., 2017. FODMAPs alter symptoms and the metabolome of patients with IBS: a randomised controlled trial. Gut 66: 1241-1251. 10.1136/gutjnl-2015-311339

Metherel, A.H., Domenichiello, A.F., Kitson, A.P., Lin, Y.H. and Bazinet, R.P., 2017. Serum n-3 Tetracosapentaenoic Acid and Tetracosahexaenoic Acid Increase Following Higher Dietary alpha-Linolenic Acid but not Docosahexaenoic Acid. Lipids 52: 167-172. 10.1007/s11745-016-4223-0

Morgan, M., 2018. BiocManager: Access the Bioconductor Project Package Repository.

Nealon, N.J., Worcester, C.R. and Ryan, E.P., 2017. Lactobacillus paracasei metabolism of rice bran reveals metabolome associated with Salmonella Typhimurium growth reduction. J Appl Microbiol 122: 1639-1656. 10.1111/jam.13459

North, J.A., Miller, A.R., Wildenthal, J.A., Young, S.J. and Tabita, F.R., 2017. Microbial pathway for anaerobic 5'-methylthioadenosine metabolism coupled to ethylene formation. Proc Natl Acad Sci U S A 114: E10455-e10464. 10.1073/pnas.1711625114

O'Brien, B.L., Hankewych, M., McCormick, D., Jacoby, R., Brasitus, T.A. and Halline, A.G.,

For Peer Review

1995. Urinary N1-acetylspermidine and N8-acetylspermidine excretion in normal humans and in patients with colorectal cancer. Dig Dis Sci 40: 1269-1274.
Palarea-Albaladejo, J. and Martín-Fernández, J.A., 2015. zCompositions — R package for multivariate imputation of left-censored data under a compositional approach. Chemometrics and Intelligent Laboratory Systems 143: 85-96. https://doi.org/10.1016/j.chemolab.2015.02.019
Parada, A.E., Needham, D.M. and Fuhrman, J.A., 2016. Every base matters: assessing small subunit rRNA primers for marine microbiomes with mock communities, time series and global field samples. Environ Microbiol 18: 1403-1414. 10.1111/1462-2920.13023
Pathi, S., Jutooru, I., Chadalapaka, G., Nair, V., Lee, S.O. and Safe, S., 2012. Aspirin inhibits colon cancer cell and tumor growth and downregulates specificity protein (Sp) transcription factors. PLoS One 7: e48208. 10.1371/journal.pone.0048208
Pessione, E. and Cirrincione, S., 2016. Bioactive Molecules Released in Food by Lactic Acid Bacteria: Encrypted Peptides and Biogenic Amines. 7. 10.3389/fmicb.2016.00876
Peters, K.M., Carlson, B.A., Gladyshev, V.N. and Tsuji, P.A., 2018. Selenoproteins in colon cancer. Free Radic Biol Med 127: 14-25. 10.1016/j.freeradbiomed.2018.05.075
Phoem, A.N., Chanthachum, S. and Voravuthikunchai, S.P., 2015. Applications of microencapsulated Bifidobacterium longum with Eleutherine americana in fresh milk tofu and pineapple juice. Nutrients 7: 2469-2484. 10.3390/nu7042469
Pires, A.S., Marques, C.R., Encarnacao, J.C., Abrantes, A.M., Mamede, A.C., Laranjo, M., Goncalves, A.C., Sarmento-Ribeiro, A.B. and Botelho, M.F., 2016. Ascorbic acid and colon cancer: an oxidative stimulus to cell death depending on cell profile. Eur J Cell Biol 95: 208-218. 10.1016/j.ejcb.2016.04.001
Quast, C., Pruesse, E., Yilmaz, P., Gerken, J., Schweer, T., Yarza, P., Peplies, J. and Glockner, F.O., 2013. The SILVA ribosomal RNA gene database project: improved data processing and web-based tools. Nucleic Acids Res 41: D590-596. 10.1093/nar/gks1219
Radenkovs, V., Kviesis, J., Juhnevica-Radenkova, K., Valdovska, A., Pussa, T., Klavins, M. and Drudze, I., 2018. Valorization of Wild Apple (Malus spp.) By-Products as a Source of Essential Fatty Acids, Tocopherols and Phytosterols with Antimicrobial Activity. Plants (Basel) 7. 10.3390/plants7040090
Rezasoltani, S., Asadzadeh Aghdaei, H., Dabiri, H., Akhavan Sepahi, A., Modarressi, M.H. and Nazemalhosseini Mojarad, E., 2018. The association between fecal microbiota and different types of colorectal polyp as precursors of colorectal cancer. Microb Pathog 124: 244-249. 10.1016/j.micpath.2018.08.035
Ridlon, J.M. and Bajaj, J.S., 2015. The human gut sterolbiome: bile acid-microbiome endocrine aspects and therapeutics. Acta Pharm Sin B 5: 99-105. 10.1016/j.apsb.2015.01.006Sam, M.R., Tavakoli-Mehr, M. and Safaralizadeh, R., 2018. Omega-3 fatty acid DHA modulates p53, survivin, and microRNA-16-1 expression in KRAS-mutant colorectal cancer stem-like cells. Genes Nutr 13: 8. 10.1186/s12263-018-0596-4
Sarabi, M.M. and Naghibalhossaini, F., 2018. The impact of polyunsaturated fatty acids on DNA methylation and expression of DNMTs in human colorectal cancer cells. Biomed Pharmacother 101: 94-99. 10.1016/j.biopha.2018.02.077
Separovic, D., Shields, A.F., Philip, P.A., Bielawski, J., Bielawska, A., Pierce, J.S. and Tarca, A.L., 2017. Altered Levels of Serum Ceramide, Sphingosine and Sphingomyelin Are Associated with Colorectal Cancer: A Retrospective Pilot Study. Anticancer Res 37: 1213-1218. 10.21873/anticanres.11436
Sheflin, A.M., Borresen, E.C., Kirkwood, J.S., Boot, C.M., Whitney, A.K., Lu, S., Brown, R.J., Broeckling, C.D., Ryan, E.P. and Weir, T.L., 2017. Dietary supplementation with rice bran or navy bean alters gut bacterial metabolism in colorectal cancer survivors. Mol Nutr Food Res 61. 10.1002/mnfr.201500905

For Peer Review

Sheflin, A.M., Borresen, E.C., Wdowik, M.J., Rao, S., Brown, R.J., Heuberger, A.L., Broeckling, C.D., Weir, T.L. and Ryan, E.P., 2015. Pilot dietary intervention with heat-stabilized rice bran modulates stool microbiota and metabolites in healthy adults. Nutrients 7: 1282-1300. 10.3390/nu7021282
Si, X., Shang, W., Zhou, Z., Shui, G., Lam, S.M., Blanchard, C. and Strappe, P., 2018. Gamma-aminobutyric Acid Enriched Rice Bran Diet Attenuates Insulin Resistance and Balances Energy Expenditure via Modification of Gut Microbiota and Short-Chain Fatty Acids. J Agric Food Chem 66: 881-890. 10.1021/acs.jafc.7b04994
So, W.K.W., Law, B.M.H., Law, P.T.W., Chan, C.W.H. and Chair, S.Y., 2016. Current Hypothesis for the Relationship between Dietary Rice Bran Intake, the Intestinal Microbiota and Colorectal Cancer Prevention. Nutrients 8: 569. 10.3390/nu8090569
Sohail, M., Rakha, A., Butt, M.S., Iqbal, M.J. and Rashid, S., 2017. Rice bran nutraceutics: A comprehensive review. Crit Rev Food Sci Nutr 57: 3771-3780. 10.1080/10408398.2016.1164120
Stark, L.A., Reid, K., Sansom, O.J., Din, F.V., Guichard, S., Mayer, I., Jodrell, D.I., Clarke, A.R. and Dunlop, M.G., 2007. Aspirin activates the NF-kappaB signalling pathway and induces apoptosis in intestinal neoplasia in two in vivo models of human colorectal cancer. Carcinogenesis 28: 968-976. 10.1093/carcin/bgl220
Suh, J.H., Makarova, A.M., Gomez, J.M., Paul, L.A. and Saba, J.D., 2017. An LC/MS/MS method for quantitation of chemopreventive sphingadienes in food products and biological samples. J Chromatogr B Analyt Technol Biomed Life Sci 1061-1062: 292-299. 10.1016/j.jchromb.2017.07.040
Sutton, S.C., LeCluyse, E.L., Cammack, L. and Fix, J.A., 1992. Enhanced bioavailability of cefoxitin using palmitoyl L-carnitine. I. Enhancer activity in different intestinal regions. Pharm Res 9: 191-194.
Sutton, S.C., LeCluyse, E.L., Engle, K., Pipkin, J.D. and Fix, J.A., 1993. Enhanced bioavailability of cefoxitin using palmitoylcarnitine. II. Use of directly compressed tablet formulations in the rat and dog. Pharm Res 10: 1516-1520.
Tamanai-Shacoori, Z., Smida, I., Bousarghin, L., Loreal, O., Meuric, V., Fong, S.B., Bonnaure-Mallet, M. and Jolivet-Gougeon, A., 2017. Roseburia spp.: a marker of health? Future Microbiol 12: 157-170. 10.2217/fmb-2016-0130
Team, R.C., 2018. R: A language and environment for statistical computing. R Foundation for Statistical Computing, Vienna, Austria.
Theodosakis, N., Langdon, C.G., Micevic, G., Krykbaeva, I., Means, R.E., Stern, D.F. and Bosenberg, M.W., 2018. Inhibition of isoprenylation synergizes with MAPK blockade to prevent growth in treatment-resistant melanoma, colorectal, and lung cancer. Pigment Cell Melanoma Res. 10.1111/pcmr.12742
Tian, R., Zuo, X., Jaoude, J., Mao, F., Colby, J. and Shureiqi, I., 2017. ALOX15 as a suppressor of inflammation and cancer: Lost in the link. Prostaglandins Other Lipid Mediat 132: 77-83. 10.1016/j.prostaglandins.2017.01.002
Tovar, J., de Mello, V.D., Nilsson, A., Johansson, M., Paananen, J., Lehtonen, M., Hanhineva, K. and Bjorck, I., 2017. Reduction in cardiometabolic risk factors by a multifunctional diet is mediated via several branches of metabolism as evidenced by nontargeted metabolite profiling approach. Mol Nutr Food Res 61. 10.1002/mnfr.201600552Tremblay, S., Romain, G., Roux, M., Chen, X.L., Brown, K., Gibson, D.L., Ramanathan, S. and Menendez, A., 2017. Bile Acid Administration Elicits an Intestinal Antimicrobial Program and Reduces the Bacterial Burden in Two Mouse Models of Enteric Infection. Infect Immun 85. 10.1128/iai.00942-16

For Peer Review

Tse, J.W.T., Jenkins, L.J., Chionh, F. and Mariadason, J.M., 2017. Aberrant DNA Methylation in Colorectal Cancer: What Should We Target? Trends Cancer 3: 698-712. 10.1016/j.trecan.2017.08.003

Tuncil, Y.E., Thakkar, R.D., Arioglu-Tuncil, S., Hamaker, B.R. and Lindemann, S.R., 2018. Fecal Microbiota Responses to Bran Particles Are Specific to Cereal Type and In Vitro Digestion Methods That Mimic Upper Gastrointestinal Tract Passage. J Agric Food Chem 66: 12580-12593. 10.1021/acs.jafc.8b03469

Ulaganathan, V., Kandiah, M. and Shariff, Z.M., 2018. A case-control study on the association of abdominal obesity and hypercholesterolemia with the risk of colorectal cancer. J Carcinog 17: 4. 10.4103/jcar.JCar_2_18

Vandeputte, D., Falony, G., Vieira-Silva, S., Wang, J., Sailer, M., Theis, S., Verbeke, K. and Raes, J., 2017. Prebiotic inulin-type fructans induce specific changes in the human gut microbiota. Gut 66: 1968-1974. 10.1136/gutjnl-2016-313271

Vu, V.Q., 2011. ggbiplot: A ggplot2 based biplot.

Walters, W., Hyde, E.R., Berg-Lyons, D., Ackermann, G., Humphrey, G., Parada, A., Gilbert, J.A., Jansson, J.K., Caporaso, J.G., Fuhrman, J.A., Apprill, A. and Knight, R., 2016. Improved Bacterial 16S rRNA Gene (V4 and V4-5) and Fungal Internal Transcribed Spacer Marker Gene Primers for Microbial Community Surveys. mSystems 1. 10.1128/mSystems.00009-15

Watson, J.A., Fang, M. and Lowenstein, J.M., 1969. Tricarballylate and hydroxycitrate: Substrate and inhibitor of ATP: Citrate oxaloacetate lyase. Archives of Biochemistry and Biophysics 135: 209-217. https://doi.org/10.1016/0003-9861(69)90532-3

Wickham, H., 2007. Reshaping Data with the reshape Package. Journal of Statistical Software 21: 1-20.

Wickham, H., 2016. ggplot2: Elegant Graphics for Data Analysis. Springer-Verlag New York. 10.1007/978-0-387-98141-3

Wilcoxon, F., 1945. Individual Comparisons by Ranking Methods. Biometrics Bulletin 1: 80-83. 10.2307/3001968

Wolffram, S., Badertscher, M. and Scharrer, E., 1994. Carrier-mediated transport is involved in mucosal succinate uptake by rat large intestine. Exp Physiol 79: 215-226.

Yang, X., Twitchell, E., Li, G., Wen, K., Weiss, M., Kocher, J., Lei, S., Ramesh, A., Ryan, E.P. and Yuan, L., 2015. High protective efficacy of rice bran against human rotavirus diarrhea via enhancing probiotic growth, gut barrier function, and innate immunity. Sci Rep 5: 15004. 10.1038/srep15004

Yilmaz, P., Parfrey, L.W., Yarza, P., Gerken, J., Pruesse, E., Quast, C., Schweer, T., Peplies, J., Ludwig, W. and Glockner, F.O., 2014. The SILVA and "All-species Living Tree Project (LTP)" taxonomic frameworks. Nucleic Acids Res 42: D643-648. 10.1093/nar/gkt1209

Yoav Benjamini, Y.H., 1995. Controlling the False Discovery Rate: A Practical and Powerful Approach to Multiple Testing. Journal of the Royal Statistical Society. Series B (Methodological) 57: 289-300.

Zarei, I., Brown, D.G., Nealon, N.J. and Ryan, E.P., 2017. Rice Bran Metabolome Contains Amino Acids, Vitamins & Cofactors, and Phytochemicals with Medicinal and Nutritional Properties. Rice (N Y) 10: 24. 10.1186/s12284-017-0157-2

Zheng, H., Yde, C.C., Clausen, M.R., Kristensen, M., Lorenzen, J., Astrup, A. and Bertram, H.C., 2015. Metabolomics investigation to shed light on cheese as a possible piece in the French paradox puzzle. J Agric Food Chem 63: 2830-2839. 10.1021/jf505878a

Zhou, Y., Tozzi, F., Chen, J., Fan, F., Xia, L., Wang, J., Gao, G., Zhang, A., Xia, X., Brasher, H., Widger, W., Ellis, L.M. and Weihua, Z., 2012. Intracellular ATP Levels Are a Pivotal Determinant of Chemoresistance in Colon Cancer Cells. Cancer Research 72: 304. 10.1158/0008-5472.CAN-11-1674

For Peer Review

For Peer Review

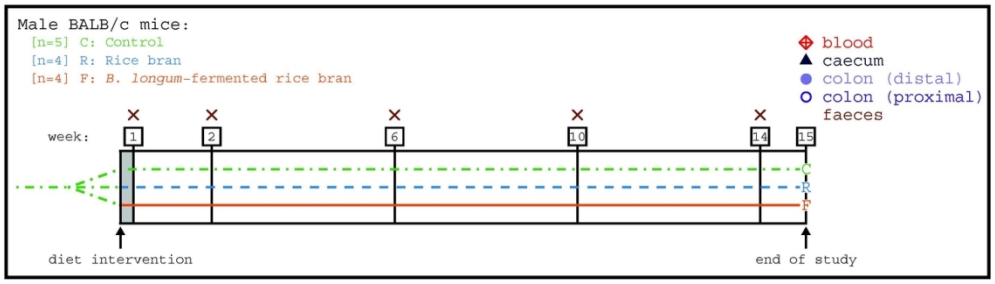

Figure 1. Study design and timeline of sampling.
Male BALB/c mice were fed control, rice bran, or *B. longum*-fermented rice bran diets for 15 weeks. Faeces, caecum, and colon were collected for both microbiota and metabolite analysis; blood was collected for metabolite analysis only.

124x37mm (300 x 300 DPI)

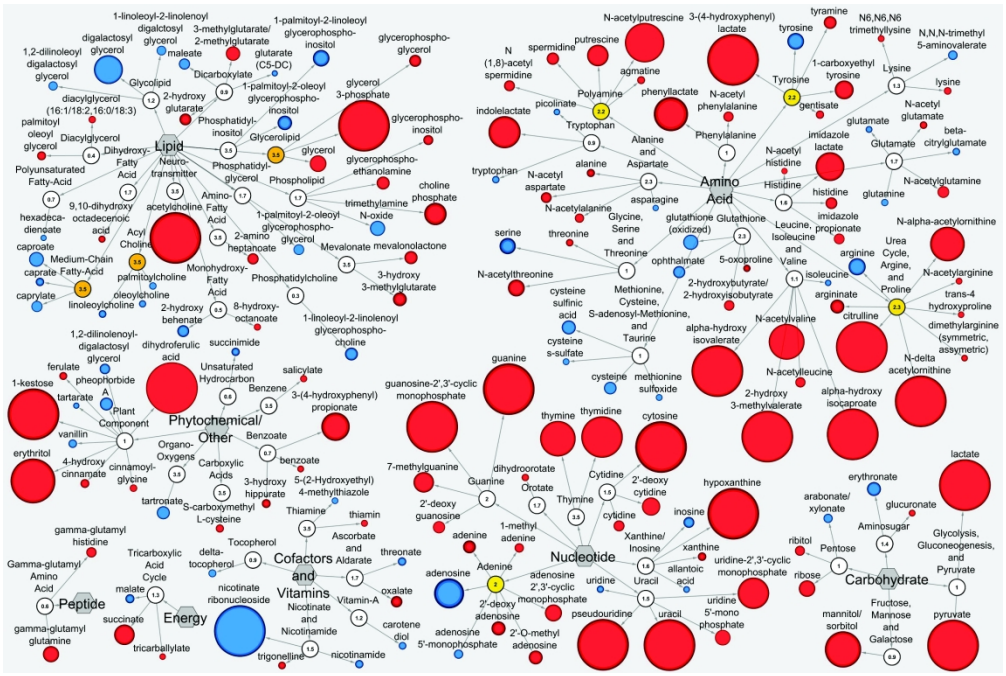

Figure 2. Fermentation with B. longum alters the rice bran food metabolome.
Metabolites that were statistically-different in abundance between *B. longum*-fermented rice bran and rice bran food metabolomes are depicted. Metabolites are organised by chemical class and further stratified by metabolic pathway, where each coloured node represents one metabolite. Node diameter reflects the magnitude of the fold abundance difference for the metabolite between *B. longum*-fermented rice bran and rice bran. Red nodes indicate metabolites that were significantly-increased in *B. longum*-fermented rice bran versus rice bran, and blue nodes indicate metabolites that were significantly-decreased in *B. longum*-fermented rice bran versus rice bran. Numbers in nodes are pathway enrichment scores.

1133x758mm (600 x 600 DPI)

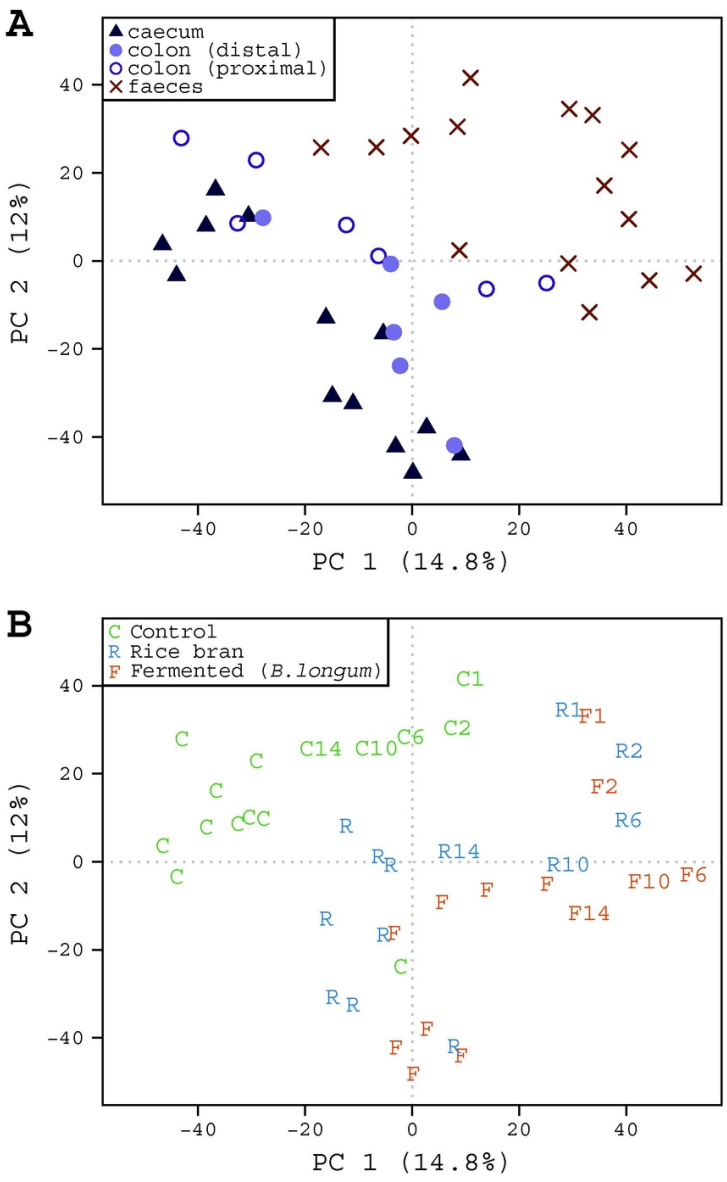

Figure 3. Healthy murine microbiomes exhibit clear separation in community composition based upon sample type and diet group.

Principal components analysis of centred log-ratio transformed absolute abundances for all sequence variants with abundance greater than two in faecal, colon, and caecum samples. Percentage values along each axis indicate the amount of variation explained by each of the first two principal components. [A] Symbols and colours denote sample type (faecal, caecum, distal or proximal colon; see key). [B] Letters and s denote mouse diet group (control, rice bran, *B. longum*-fermented rice bran; see key).

74x119mm (300 x 300 DPI)

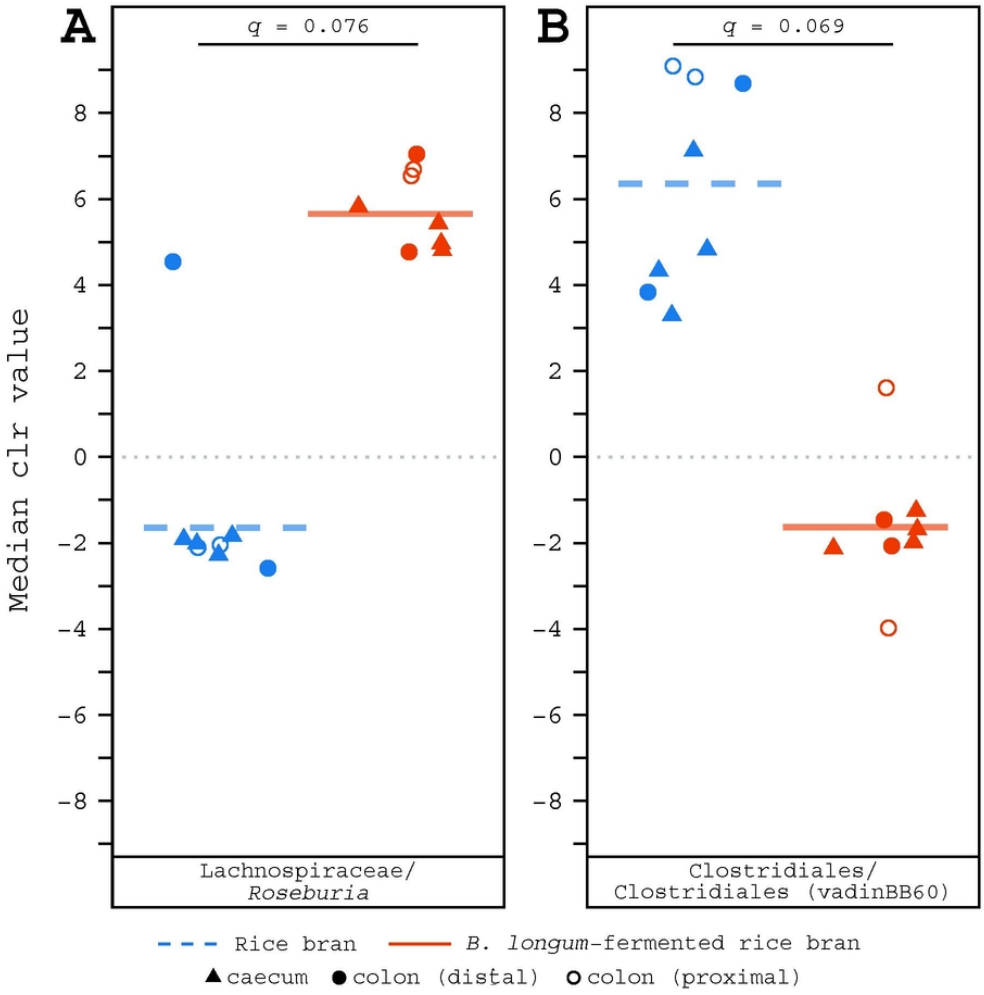

Figure 4. Consumption of *B. longum*-fermented rice bran versus rice bran minimally alters the caecum and colon microbiomes of healthy mice.

[A-B] Strip charts of median centred log-ratio values for two sequence variants considered to be differentially abundant (q<0.1) between microbiomes from mice fed a *B. longum*-fermented rice bran or a rice bran diet. Symbols denote sample type (caecum, distal or proximal colon; see key); line style and colours denote mouse diet (rice bran, *B. longum*-fermented rice bran; see key). Lines represent the median clr value for all samples within a diet group, while points represent the median clr value for each individual sample. Sequence variant taxonomic identities from Greengenes and SILVA databases are indicated on the x-axis styled as Greengenes/SILVA.

77x77mm (300 x 300 DPI)

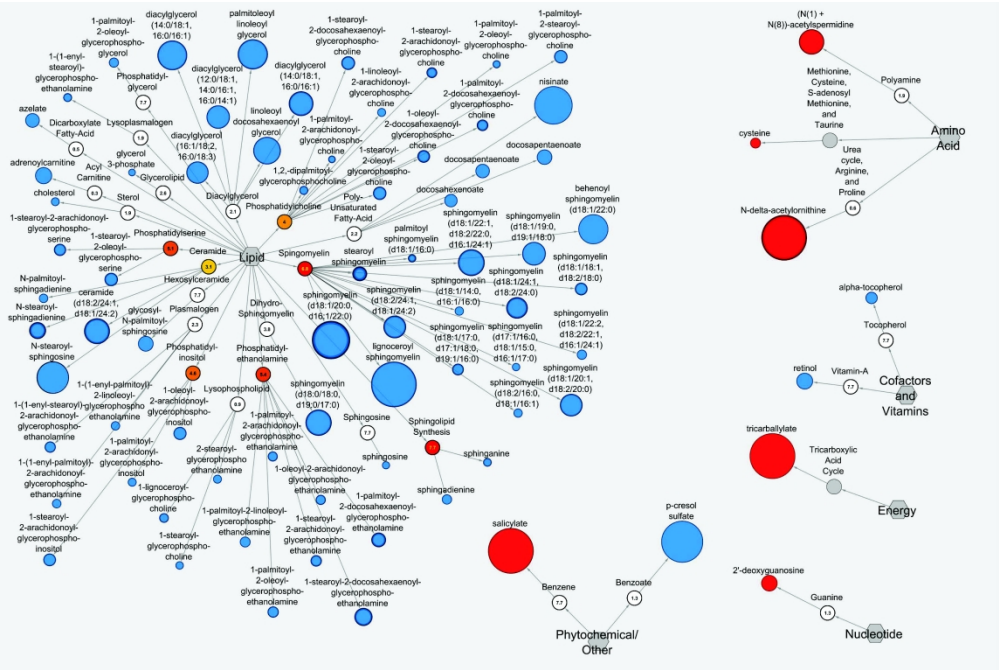

Figure 5. Consumption of *B. longum*-fermented rice bran versus rice bran alters the colon tissue metabolome of healthy mice. Metabolites that were statistically-different in abundance between *B. longum*-fermented rice bran versus rice bran-fed mice are depicted. Metabolites are organised by chemical class and further stratified by metabolic pathway, where each coloured node represents one metabolite. Node diameter reflects the magnitude of the fold abundance difference for the metabolite between *B. longum*-fermented rice bran and rice bran. Red nodes indicate metabolites that were significantly-increased in the colon of *B. longum*-fermented rice bran fed mice versus rice bran fed mice, and blue nodes indicate metabolites that were significantly-decreased in *B. longum*-fermented rice bran versus rice bran. Numbers in nodes are pathway enrichment scores.

850x569mm (600 x 600 DPI)